DEPARTMENT OF MINERALS AND ENERGY

BUREAU OF MINERAL RESOURCES, GEOLOGY AND GEOPHYSICS

Record 1976/61

WEWAK GEOPHYSICAL SURVEY FOR GROUNDWATER, PNG 1973

by

G.R. Pettifer and F.J. Taylor

Record 1976/61

WEWAK GEOPHYSICAL SURVEY FOR GROUNDWATER, PNG 1973

by

G.R. Pettifer and F.J. Taylor

CONTENTS

ILLUSTRATIONS

SUMMARY

A geophysical survey for groundwater in Wewak has indicated a minimum depth of 50 m to weathered mudstone bedrock and a maximum depth of between 110 and 160 m. Evidence is strong for thinning of the coastal plain sediments west of Wewak, but test drilling is recommended to check these conclusions

Resistivity probes in the area of the Wewak fire station bore suggest that further groundwater supplies can be expected if the bore is deepened. Low-resistivity layers detected at depths of between 10 and 20 m indicate old brackish-water swamp surfaces. The golf course and possibly the teachers' college are two areas where the resistivity results suggest possible groundwater supplies at depths less than 50 m.

1. INTRODUCTION

The Public Works Department (PWD) of Papua New Guinea is proposing a groundwater reticulation system for the domestic supply of Wewak, with an anticipated demand of 500 000 gallons per day in the 1980s. In order to locate a reliable source of groundwater, PWD undertook an investigation of the groundwater resources, this included a geological survey of the town area and a drilling program of six exploratory bores. The bores failed to penetrate the Recent coastal plain sediments to the weathered mudstone bedrock. Five out of the six bores struck water, but only two of them were successfully completed and pump tests carried out. The geological investigation (Harris, 1971) outlined the problems and potential for development of a groundwater supply, and recommended a geophysical survey to measure the thickness of the unconsolidated coastal plain sediments and to indicate possible aquifers.

A party from the Engineering Geophysics Group of the Bureau of Mineral Resources (BMR) - consisting of F.J. Taylor (party leader), G.R. Pettifer (geophysicist), and R.D.E. Cherry (shooter) - assisted by G.M. Pounder (technical assistant, Geological Survey of PNG), carried out a geophysical survey in April and May 1973. Seismic and resistivity methods were employed to determine the thickness of the coastal plain alluvium and the distribution of possible aquifers.

Wewak, 95 km west of the mouth of the Sepik River, is situated on a swampy narrow coastal plain on the north coast of New Guinea in the West Sepik District. Present water supplies are from rainwater (average rainfall 235 cm per year) and from some private shallow wells and bores. The Cape Moem Barracks and Wewak hospital are supplied from chlorinated surface-water storages. The existing boreholes show the sediments to be mainly impermeable silts and clays with some fine to medium sand aquifers. Shallow aquifers are contaminated by permeating salt water, and some by the bacterium Escherichia cholii. Boreholes drilled near sago palm and mangrove swamps produce brackish, organic-smelling water.

A short seismic survey was also carried out at the Nagam River crossing on the Wewak-Maprik road for PWD. The results of this work are appended with this report (Appendix 4).

2. GEOLOGY AND HYDROLOGY OF WEWAK

This account is taken from a hydrogeological report on the Wewak area by Harris (1971). Investigations for engineering materials have also been undertaken in the area (Braybrooke, 1969). Plate 1 shows the geology of the area.

Wewak lies on a coastal plain which varies in width from 0.4 to 8.5 km and lies at the base of the foothills of the Prince Alexander Mountains. The town of Wewak lies on a raised coral reef (Wewak Point). Several other coral headlands - Cape Wom, Cape Boram, and Cape Moem - extend into the Bismarck Sea and partly enclose sheltered bays.

Pliocene mudstone, marl, and greywacke, commonly deeply weathered, form the foothills south of Wewak; the rocks dip between 15° and 40° north. An exploratory (PWD 1, Plates 1 and 2) was drilled on bedrock and proved weathered mudstone to at least 27 m below the surface. The Pliocene rocks show little primary or fracture permeability, and the groundwater potential of the bedrock is considered to be low.

Plio-Pleistocene coral limestone crops out on the headlands and in Kreer subdivision above the PWD compound. At Wewak Point the limestone is 30 m thick and dips at about 10° north. PWD 3 (Plate 1), near Wewak airstrip, penetrated limestone to a depth of 15 m below the surface. Water of low quality was encountered at 11 m; however, pumping tests showed the supply to be of low specific capacity. A high-capacity shallow well is located within the Army Base on Cape Moem in the raised coral limestone (Army Base Engineer, pers. comm.).

South of Wewak airstrip at Boram, Pleistocene pebbly sand deposits form a kunai-covered ridge. Smaller deposits (not indicated in Plate 1) also occur at the base of the raised coral limestone near Kreer, and near the Brandi River in the foothills behind the army base. Except for the deposit at Kreer, the Pleistocene pebbly sand deposits are mostly above the water-table.

The main aquifers in the Wewak area occur in the Recent sediments which form the coastal plain. The sediments extend to an unknown depth, but have been proved to at least 51 m in the Mobil bore. The surface deposits, which support large areas of freshwater sago palm and saltwater mangrove swamps, consist of narrow beach sand ridges along the coast; they are commonly underlain by a grey organic silty fine sand further inland. Farther inland again, on land of higher elevation, silty clay is common at the surface. Below 6 m, the surface deposits generally grade into dark grey silts with beds of clay and sand, in which shelly horizons are common. At depth in some boreholes (exploratory bore PWD 4 and Wewak Hotel bore, Plate 2), the alluvium grades into fine to medium-coarse sands. Difficulty was encountered in drilling PWD 4, in which sands encountered between 25.5 and 36.5 m below sea level were under high hydrostatic pressure and filled the hole;

the water was unacceptably cloudy owing to a high content of clay particles in suspension, and the hole was subsequently abandoned. A similar difficulty was encountered nearby in PWD 5.

At least ten boreholes have been drilled in the coastal plain sediments and five have successfully located groundwater. At Wewak Hotel, on Wewak Point, water is pumped from a fine-medium sand aquifer 17 m below sea level and less than 100 m from the sea. The aquifer is partly confined, and a steady flow of fresh groundwater seawards prevents salt-water contamination; however, the severe drought of 1972, and overpumping of the bore, resulted in sea-water contamination of the aquifer, and the resistivity of water samples taken at the time of the survey reflect this (Appendix 1). A bore drilled at Boram police barracks, east of Wewak airstrip terminal and 200 m inland from the coast, encountered salt water at a depth between 4.5 and 11 m below sea level. Bores drilled on reclaimed swamp yield brackish, organic-smelling water (Mobil bore, Plates 1 and 2, Appendix 1). A bore drilled for the Wewak abbatoirs west of Wewak encountered water at 17 m depth; however, contamination of the water by E. cholii renders it unsuitable for use at the meatworks.

PWD 3 and Wewak fire station bore (Plates 1 and 2) have encountered high specific-capacity (250 gph per foot of drawdown) aquifers at depths of 20 to 24 m, and these areas appear to provide the best prospects for immediate development of groundwater supplies. Elsewhere, pumping tests on PWD 2, Wewak abbatoir bore, and Wewak Hotel bore show specific capacities of less than 90 gph per foot of drawdown. The low specific capacities reflect the fine grainsize and low permeabilities of the coastal plain sediments.

Shallow wells at Wewak Cordials, Windjammer Motel, the Army Base, Wewak village, and Fiske have encountered fresh water at depths of less than 4.5 m. Recharge of the wells and the deeper coastal plain aquifers is from infiltration of surface streams and rainwater.

Water quality varies considerably. However, the water is generally hard: good-quality water for the Wewak area has hardness values as high as 500 ppm ($CaCO_3$ equivalence). The water generally has high concentrations of magnesium ions (49-100 ppm), which gives it a slightly bitter taste, and bi-carbonate ions (160-750 ppm). The resistivity of the ground-water can be expected to vary from 0.16 ohm-m (for sea water), through 2-3 ohm-m for brackish-organic water, to 10-14 ohm-m for good quality groundwater (Appendix 1).

3. METHODS AND EQUIPMENT

3.1 Seismic method

For the seismic work, refraction and shallow reflection methods were used. Two seismic depth probes were carried out: one at the southern side of Wirui airstrip; the other on a sheltered beach on the western side of Cape Moem (Plate 1).

At Wirui airstrip, 24 geophones were spaced at 15-m intervals, and refraction shots were fired 16 m offset. Noise from aircraft and nearby light industrial workshops, and the severe attenuation of the seismic signal within the unconsolidated alluvium, prevented larger offsets being used.

At Cape Moem, geophones were spaced at 10-m intervals in a total spread length of 230 m. For the refraction shots, offsets of 50, 200, 530, 1100, and 2000 m were used. All shots were fired on the northern side of the spread, as dense jungle swamp and narrowness of the coastal plain prevented reverse shooting. A small reflection shot was fired 30 m offset from the centre of the spread.

The standard BMR 24-channel shallow seismic refraction system (SIE Dresser Co.) and 8 Hz GSC-20D (Geospace Corporation) geophones were used throughout the survey.

3.2 Resistivity Method

An Evershed and Vignoles' Geophysical Megger (0-30 ohm, AC) was used to measure Earth resistances. The instrumental accuracy was found to be better than 3 percent for resistances above 0.1 ohm, but deteriorated to 5 percent at 0.05 ohm and 10 percent or more for still lower values.

The Wenner configuration was used throughout the survey: four electrodes are placed at equal spacings (a), and the spacing is increased successively, allowing increasingly deeper penetrations.

The Wenner tripotential method (Carpenter & Habberjam, 1956) was used to determine and reduce lateral effects that produce a deviation from values which are permissible assuming resistivity varies with depth only. In the tripotential method, using four electrodes, three different combinations of current (C) and potential (P) electrodes are possible as outlined in Table 1. These three combinations, denoted α, β, and γ give three different values of resistance (R) and resistivity (ρ). The resistance (R) is the ratio of voltage

(ΔV) measured between the two potential electrodes to the current (I) passing between the two current electrodes. The resistivity (ρ) is the product of the resistance and a geometrical factor (G), which varies for each electrode configuration and is directly proportional to the electrode spacing (a).

Table 1

Configuration	Electrode Arrangement	Resistivity	Geometrical Factor
α	CPPC	$\rho_\alpha = G_\alpha R_\alpha$	$G_\alpha = 2\pi a$
β	CCPP	$\rho_\beta = G_\beta R_\beta$	$G_\beta = 6\pi a$
γ	CPCP	$\rho_\gamma = G_\gamma R_\gamma$	$G_\gamma = 3\pi a$

Habberjam (1967), in verifying the law of reciprocity in resistivity work, showed that for the tripotential method the additive law (equation 1) applies:

$$R_\alpha = R_\beta + R_\gamma$$

Measurement of the three readings provides a check on instrumental and reading errors. For this survey, only R_α and R_γ were measured, as the Megger was incapable of reading the low voltages obtained with the β configuration (dipole-dipole). Thus the instrumental and reading errors (generally better than 3%) were tolerated. Habberjam concluded that the effects of lateral inhomogeneities are likely to be the main source of perturbation in the relation between R_α and R_γ.

In the fieldwork a switching device was used between the instrument and the electrodes, to facilitate measurements by switching between the α and γ configurations.

Habberjam & Watkins (1967) showed that for a layered resistivity medium a theoretical relation exists between the resistivities measured on the α and γ configurations; and that lateral changes causing deviations from this theoretical relations, will be disclosed by field measurements. Habberjam & Watkins (1967) described a method of minimum adjustment of the field data to extract from the field data the maximum part which can be reconciled with a purely depth variation of resistivity. Also, from the departures from the theoretical relations in the field data, a measure of the lateral effects detectable in each depth probe is obtained.

Appendix 2 summarizes the theory of the tripotential method. The adjustment was carried out by a computer program which produced a best-fitting layered-medium curve. This curve was then interpreted in the normal manner using two-layer curve-matching techniques. The final interpretation was obtained from an iterative computer modelling program (Vozoff, 1958) which modified the two-layer curve-matching interpretation to obtain an interpretation which agreed best with the adjusted field data.

In the Wewak area, fifteen depth probes were carried out (Plate 1), with a maximum electrode spacing of 256 m being obtained. Generally, however, because of the low resistivities in the area maximum electrode spacings of only 128 m or less were possible. To comply with the adjustment method, standard electrode spacings were used in the field. Two concurrent geometric series of 0.5, 1, 2, 4, 8, 16, 32, etc., and 1.5, 3, 6, 12, 24, 48, etc., (all values in metres) were employed for each depth probe.

Water samples were taken from boreholes and surface waters in the Wewak area, and resistivities were measured in the BMR mud-cell using an Evershed and Vignoles Megger Earth Tester. Appendix 1 shows the results of the resistivity measurements.

4. RESULTS AND INTERPRETATION

4.1 Seismic Results

Table 2 summarizes the results of the seismic depth probe at Cape Moem Army Barracks (Plate 1).

Table 2

Seismic refraction results - Cape Moem

Depth (m)	Thickness (m)	Velocity (m/s)
0-3	3	300
3-50	47	1700
50-110 (± 10)	60	1900
110- ?		2200 - 2300

A strong reflection recorded from a depth of 110 m is almost certainly the 1900-2200 m/s interface. The 1700 m/s velocity represents the unconsolidated Recent sediments and corals.

Table 3 summarizes the results from Wirui airstrip.

Table 3

Seismic refraction results-Wirui airstrip (Plate 1)

Depth (m)	Thickness (m)	Velocity (m/sec)
0-3	3	300
3-49	46	1700

Evidence of a reflection from a depth of 160 m at Wirui airstrip was suggested by the reflection results; however, noise precluded large offsets from being used to determine a deeper refractor than the 1700 m/s velocity layer and the reflection could not be correlated with a refracting horizon.

On the seismic evidence alone, two interpretations of the results are possible. The 1900 m/s refractor might represent weathered mudstone, with the 2200-2300 m/s material being fresh Pliocene mudstone. The effective thickness of recent sediments would then be at least 49 m at Wirui airstrip and 50 m at Cape Moem. Seismic refraction work on the Pliocene bedrock for the Nagam River bridge site, 25 kms from Wewak, indicated a maximum velocity of 1600 m/s for weathered mudstone at the surface (Appendix 4). More probably the 1900 m/s material is both consolidated Recent sediments and Pliocene weathered mudstone, and the two are indistinguishable. Experience in Recent alluvial environments in Papua New Guinea with seismic work (Bishop, Pettifer, & Polak, in prep.) suggests gradation of alluvial velocities from 1700 to 1900 m/s at depths of 50-60 m.

The seismic results suggest that the Recent coastal plain sediments are between 50 and 110 m thick at Cape Moem (Plate 1), and at least 49 m but probably less than 160 m at Wirui airstrip. The Cape Moem depth probe was located 2.1 km from the nearest outcrop of Pliocene, whereas Wirui airstrip is 1.5 km from outcrop. As a deeper refractor was recorded at Wirui airstrip the Recent coastal plain sediments may be thicker towards Wewak township.

4.2 Resistivity Results

4.2.1 Experiences with the Wenner Tripotential method in the Wewak area

Plate 1 shows the location of the fifteen resistivity depth probes, and Plates 3 to 17 presents the results for each depth probe.

4.2.1.1 Presentation of depth probes

The results are plotted in the standard manner on a bilogarithmic scale, showing resistivity (ρ) in ohm-metres as the abscissa, and electrode spacing (a) in metres as the ordinate. The field data for both the α (shown as circles) and the γ (shown as crosses) configurations are presented. The dashed curve represents the adjusted and smoothed normal Wenner curve, and the solid curve is the curve of the final computer model solution. The layered model solution is shown as a histogram plot of resistivity versus depth, and the Lateral Inhomogeneity Ratio (L.I.R., Appendix 2) versus spacing plot is included to show qualitatively the degree of lateral variations.

4.2.1.2 Significance of LII values

Table 4 lists the Lateral Inhomogeneity Index (LII, Appendix 2) for each depth probe. Habberjam & Watkins (1967) classified LII values into three arbitrary categories; low LIIs (less than 0.2), intermediate LIIs (0.2 to 0.5) and high LIIs (greater than 0.5), and suggested that for high LII values the layered model interpretation is of questionable value.

The results suggest appreciable lateral variations in resistivity for most of the locations investigated with the resistivity method. Vincenz (1968), in using the tripotential method in a cavernous fissured limestone environment where lateral resistivity variations are common, concluded that only lateral variations of dimension of the order of the length of the electrode spread were significant, with small near-surface inhomogeneities being detected at closer spacings and increasingly larger inhomogeneities being detected with increasing electrode spacing. For larger electrode spacings the smaller inhomogeneities have little influence, and a high value of the LIR might reflect either broader variations in the surface layer or in layers at depth.

Table 4

Lateral Inhomogeneity Index values - Wewak depth probes

Depth Probe	LII	Classification
1	0.30	Intermediate
2	0.14	Low
3	0.40	Intermediate
4	0.17	Low
5	0.59	High
6	1.29	High
7	0.22	Intermediate
8	0.46	Intermediate
9	0.98	High
10	0.61	High
11	0.04	Low
12	0.45	Intermediate
13	0.42	Intermediate
14	3.71	High
15	4.36	High

Depth probes 5 and 6 at Wirui airstrip, 14 and 15 at Wewak airstrip, and, to a lesser extent, 9 and 10 near the teachers' college show high LII values.

Also, depth probes 5, 6, 9, 10, 14, and 15 are characterized by the fact that the tripotential reduction and smoothing process has tended to increase the depth to the low-resistivity layer and to introduce an intermediate layer. This phenomenon was investigated (Appendix 3) after the survey, and the reasons for it are not altogether clear. The intermediate layer, if present, affects the interpretation of the subsurface hydrological conditions, particularly in the teachers' college area (depth probe 9 and 10). As a result of the further investigations the conclusion has been drawn that the geophysical megger used is not sufficiently accurate for the tripotential method, particularly in a low-resitivity area such as Wewak, where measured resistances are low especially at larger electrode spacings. The phenomenon of high LII being associated with large resistivity contrasts and the

introduction of an intermediate layer has also been verified in a beach environment (Appendix 3) using a different instrument. This suggests that the phenomenon is not due to instrumental error. Because the measured LII values were high, any interpretation of either the raw field data or the smoothed data in terms of horizontal layering must be considered unreliable for these six depth probes.

The high LII values might be attributed to the fact that the airstrips and roads in these locations are constructed from crushed coral limestone (coronus), which shows high and variable resistivities (350-5000 ohm-m). The coronus is generally underlain by lower-resistivity material varying from brackish water saturated clays (0.35-2.30 ohm-m), particularly beneath the airstrips, to sandy clays (9-20 ohm-m) at the teachers' college. The high resistivity contrast between the coronus and the underlying sediments, and the high variability of the coronus and the underlying sediments, suggest that the high LII values for these probes are due to variations in thickness and resistivity of the surface coronus layer.

4.2.1.3 Other difficulties

In addition to the generally high lateral variations, several difficulties encountered in both the fieldwork and interpretation are important in considering the reliability of the resistivity survey results.

The generally low resistivities of the sediments in the Wewak area, and particularly the occurrence of thin low-resistivity layers near the surface, limited depth penetration with the low-powered resistivity equipment used in the survey.

In addition, depth penetrations were further hampered in the populated areas because maximum desirable electrode expansions could not be attained. All available land not covered by swamp was heavily populated. Open areas, such as the airstrip, are generally located on reclaimed swamp, and as groundwater development is recommended only away from swamp areas (Harris, 1971) the survey was severely limited operationally as a result of this.

In the interpretation, the large changes from high surface resistivities to low resistivity underlying layers at depth often suppress the effects of intermediate layers. The interpretations carried out used models of four to six layers, and in some cases more than six layers are suggested; however, the uncertainity in interpretation increases with the number of layers.

The Wewak area is considered particularly unsuitable for a resistivity survey for these reasons. In many cases it was found that a combination of these difficulties resulted in little being added to the knowledge of the subsurface conditions.

4.2.2 Resistivity/lithology relationship - Wewak area

Table 5 shows resistivities and interpreted lithologies in the Wewak area.

Table 5 - Resistivities Wewak Area

Resistivity (ohm metres)	Interpreted lithology
35-230	Soil
350-5000	Dry coronus (surface material)
40-50 (?)	Coral
1	Salt-water-bearing formation
1-5	Brackish-water-bearing formation
5-10	Predominantly clay-bearing material, weathered mudstone
60-250	Fresh mudstone (Pliocene)
10-50	Clay, sands, and silts (lower resistivities indicate higher clay contents)

The above classifications are generalized only, and a finer classification of the coastal plain clays, sands, and silts is not possible because of the generally high clay contents. Calculation of porosities from the resistivities are also generally meaningless because of the high clay content of the sediments.

4.2.2 Correlation of depth probes and existing boreholes

Depth probes 1 (PWD 1), 7 (Wewak Point), 12 (fire station/Mission Point Wharf), and 14 (PWD 3) were carried out near boreholes, and enable some correlation between resistivities and sediment type.

4.2.2.1 Depth probe 1 and PWD 1

Depth probe No. 1 (Plate 3) was carried out on the weathered mudstone bedrock near PWD 1 and indicated low resistivity material (7-8 ohm-m) extending to a depth of 160 m. This is interpreted as weathered mudstone. A 60 ohm-m layer below 160 m almost certainly corresponds to the fresher Pliocene mudstone. These great weathering depths may account for the observed differences in depths of the two reflectors in the seismic work (section 4.1) at Cape Moem and Wirui airstrip.

4.2.2.2 Depth probe 7 and Wewak Hotel bore

The fine to medium sand below sea level at Wewak Hotel correlates with a resistivity of 9-ohm-m in depth probe 7 (Plate 9), but here the correlation must be considered tentative as the depth probe was carried out in a populated area with grounded structures, on a raised coral pinnacle near low resistivity sea water. The LIR plot (Plate 9) reflects the scatter of the field data. Depth probe 7 results suggest that the salt-water intrusion into the aquifer at Wewak Point is not extensive, as no definite low-resistivity layer (1-5 ohm-m, Table 5) indicating brackish water was revealed.

4.2.2.3 Depth probe 12 and fire station bore (section EF)

Depth probe 12 (Plate 14) on section EF (Plate 18), near the fire station bore on the Mission Point Wharf road shows a 12-ohm-m layer extending from 0.7 m beneath a salt-water surface layer to a depth of 11 m. At 11 m, water was struck, and the borehole log (Plate 2) shows a brown clayey sand and gravel correlating with the 12 ohm-m layer. Below, 11 m the main aquifer of fine to medium sand shows a resistivity of 19 ohm-m. The interpretation of depth probe 12 indicates the 19 ohm-m layer extending to a depth of 64 m and suggests that further sands would be encountered below the present depth of the fire station bore. The lower resistivity 3.2-ohm-m layer encountered below 64 m may represent weathered mudstone; however, the great lateral changes evident at electrode spacings greater than 8 m (Plate 14) suggests that the influence of the nearby sea and mangrove swamp may affect the field data, and here the interpretation is uncertain. If the interpretation is correct, then the weathered bedrock must deepen rapidly at the foot of the Pleistocene raised coral reef at Kreer. The smoothed resistivity curve for depth probe 12 suggests small variations in the 19 ohm-m layer, and may indicate alternating sand and clay beds. The fire station bore encountered silty clay at the bottom of the hole. Calculation of porosity from the resistivity of the sediments using the

standard formula (Wiebenga & Jesson, 1962), $Ro = R_w/\emptyset^{1.25}$ (where Ro is formation resistivity, Rw is the water resistivity, and $\emptyset$ is porosity expressed as a fraction), with Ro equal to 19 ohm-m and Rw equal to 13.4 ohm-m (Appendix 1), gives a value of 76 percent, which is unrealistically high. Todd (1959) cites values in the range of 35-40 percent for fine to medium sands. This indicates the high clay content of the sands in situ in the fire station area. Computations of permeabilities of the aquifer from sieve analysis (Harris, 1971) using empirical formulas (London, 1952) yield wildly varying estimates. The calculations of permeability are sensitive to errors in estimation of the porosity (Bear, 1972), and, as porosity cannot be reliably estimated from the resistivity results, no calculations of permeability are made in this report.

4.2.2.4 Depth probe No. 14 and PWD 3

PWD 3 is located near depth probe 14 (Plate 16). The results show a low-resistivity layer (0.5 ohm-m) between 14 and 17 m depth; water was struck at 11 m and the results indicate brackish or salt water at depth. The grey fine sand aquifer correlates with a layer of 10 ohm-m below 17 m. Depth probe 14 shows a high LII value (Table 4; Appendix 2) of 3.71 owing to high-resistivity surface coronus, and the interpretation must be considered tentative

4.2.3 Interpretation and Cross Sections

In the discussion of the results, three principal cross-sections are considered. These are shown in Plate 18. Plate 1 shows the location of the cross-section lines. Section AB extends from bedrock through depth probes 9 and 10, PWD 5, depth probe 8, and depth probe 7 at Wewak Point. Section CD extends from bedrock through depth probes 1, 2, 3, and 4 to the sea. Section EF, which passes through the Fire station bore has been discussed. (Section 4.2.2.3).

4.2.3.1 Section AB

Section AB, passes from PWD 1 through the teachers' college to Wewak Point. Depth probe 1 shows 160 m of weathering in the mudstone. The high-resistivity (60 to 250 ohm-m) layer, which is interpreted as representing the fresh mudstone, is detected near depth probes 9 and 10 at depths between 114 and 155 m. Depth probe 8 (Plate 10) shows very large lateral effects at the larger spacings, with very low resistivities detected on the configuration. This probe was carried out in an area close to brackish swamps and electrically grounded fences, and the interpretation of the deeper parts of the section is uncertain.

No reliable evidence of a high-resistivity bedrock layer was found in depth probe 7 on Wewak Point. A 250 ohm-m layer is interpreted by the computer program at a depth of about 45 m below sea level. However, this value of resistivity of the layer is probably an extreme upper value. Further, the presence of this layer must be in doubt because of the large topographic effect of Wewak Point. The tripotential method cannot remove lateral effects which occur parallel to the line of the electrical sounding, and the results cannot be diagnostic of the total topographic effect of Wewak Point.

The weathered mudstone layer of resistivity 7-8 ohm-m has little resistivity contrast with the typical sediment resistivities in the Wewak area, and its correlation along section AB is uncertain also.

On section AB in the teachers' college area, depth probes 9 and 10, although showing large distortion owing to the near-surface high-resistivity coronus, indicate resistivities of between 9 and 20 ohm-m at depths between 4 and 155 m. The 4 ohm-m layer at a depth of 58 m on depth probe 10 may represent the weathered mudstone. Depth probe 8 indicates a 1.8 ohm-m layer extending from 7 to 27 m depth. Depth probes 9 and 10 suggest shallow groundwater supplies, but this interpretation must be in doubt because of the high LII. Also as this area is close to PWD 4 and 5, where drilling difficulties were encountered with sands under hydrostatic pressure and fine clay particles in suspension in the water (section 2), development of a groundwater supply from this area may not prove feasible.

4.2.3.2 West of Wewak

2.5 km west of section AB, at depth probe 11 (Plate 13), at Wariman Creek bridge, a 24-ohm-m layer is indicated between 4 and 27 m depth. It is immediately underlain by a low-resistivity (3 ohm-m) layer which extends to a depth of 69 m. The very high-resistivity (640 ohm-m)layer at a depth of 69 m almost certainly represents unweathered mudstone, and the depth of the coastal plain sediments may be as little as 27 m in this area if the 3 ohm-m layer is interpreted as representing weathered bedrock. The interpretation of this depth probe is considered to be reliable evidence for shallowing of the Pliocene bedrock west of Wewak where the coastal plain widens. If this is so, then faecal contamination of the groundwater supply west of the Wewak, as observed in the Wewak abbatoir bore (section 3, Plate 2), may be more widespread, because of the very shallow depths of the groundwater storages over this widely populated area.

4.2.3.3 Wewak and Wirui Airstrip areas

Between sections AB and CD (Plates 1 and 18) depth probes 5 (Plate 7) and 6 (Plate 8) at Wirui airstrip suggest the presence of low-resistivity layers at depths of 10 to 19 m. Similar conditions are evident in depth probes 14 (Plate 16) and 15 (Plate 17) in the Boram area. The low resistivities represent salt or brackish water layers, and suggest either sea-water intrusion - as in depth probe 15 at Wewak airstrip, where a 0.7 ohm-metre layer is encountered at 17 m depth (see also Boram Police Barracks bore, section 2, Plate 2) - or, for of very thin layers (less than 3 m), old surfaces of deposition. The thin salt-water layers are probably the connate waters of old swamp surfaces. There is some suggestion of deeper occurrences of these thin low-resistivity layers in most of the resistivity depth probes, but the resolving power of the depth probe method used on the survey is limited owing to the density of data points and observed lateral variations.

4.2.3.4. Section CD

In section CD (Plate 18), fresh bedrock is detected by resistivity depth probing only at outcrop (depth probe 1). The seismic results at Wirui airstrip (projected on section CD) suggests fresh bedrock depths of 160 m near depth probe 3 (section 4.1), with weathered bedrock occurring at least 50 m below the surface. Weathered mudstone is at least 15 m deep in depth probe 2 (Plate 4). A resistivity of greater than 50 ohm-m is interpreted at a depth of 24 m in depth probe 4 (Plate 6) it the golf course area. This resistivity may represent either dry coral (Table 5) or a clean sand or porosity 30 percent. Between 12 and 24 m, brackish clays (2.4 ohm-metres) occur. The indication of the 50 ohm-m layer is very definite, and a drill hole is recommended to check the resistivity results on the golf course. Groundwater development in this area may be prevented, however, because of the proximity of the sea and the danger of salt-water intrusion. Elsewhere in section CD the resistivity indicates high clay contents in the sediments.

5. CONCLUSIONS

The geophysical survey, particularly the resistivity survey, has been confined to populated areas away from existing swamps. This has limited the operation of the survey and the interpretations of the results. The resistivity equipment used in the resistivity survey is of limited power and accuracy, and this proved a limitation in the Wewak area. The low resistivities and high lateral variability of the sediments in the Wewak area are evident in the resistivity data, and introduce

some difficulties in interpreting the results. The Wenner tripotential resistivity method has been used to reduce lateral effects which are inconsistent with the theoretical model of a layered medium, and the conclusions of this report are based on the interpretations made from the adjusted and smoothed field data (Appendix 2). The seismic operations were limited to two areas, and conclusions drawn from the deep refraction data are based on travel time information obtained by shooting in one direction only.

With these considerations in mind, several conclusions can be made from the survey results.

5.1 Minimum depths to weathered bedrock appear to range from 50 m at Cape Moem and Wirui airstrip to possibly 58 m in the area of the teachers' college. West of Wewak, on Wariman Creek, weathered bedrock depths of 27 m are interpreted. Fresh bedrock depths are interpreted at a depth of 160 m at outcrop, 110 m at Cape Moem, possibly 160 m at Wirui airstrip, and 70 m west of Wewak. Evidence is strong for a thinning of the coastal plain sediments west of Wewak township. Test drilling is recommended in a suitable area to check these conclusions.

5.2 Low-resistivity layers at depths of between 10 and 20 m have been detected beneath the two airstrip areas, and some depth probes suggest evidence of low-resistivity layers at greater depths; however, the resolving power of the depth probing method used is too limited to detect the deeper low-resistivity layers with any certainty. It is suggested that the thin layers may represent the connate salt waters of old swamp surfaces. Sea-water intrusion is evident beneath Wewak airstrip at Boram in depth probe 15.

5.2 Results of a depth probe at Wewak Point suggest that no extensive sea-water contamination of the aquifer has occured, as no definite low-resistivity layer was detected.

5.3 Depth probe 4 at the golf course indicated a high-resistivity layer (50 ohm-m) at a depth of 24 m. This resistivity may correspond to either buried coral or a clean fine to medium sand. This area is recommended as an area for test drilling by future drilling programs.

5.4 Resistivity results on the Mission Point road indicate a 19-ohm-m layer extending from the water-table to a depth of 64 m. Evidence for alternating clay and sand layers is also suggested by the resistivity results. This suggests that deepening of the fire station bore may encounter further aquifers.

6. REFERENCES

BEAR, J., 1972 - DYNAMICS OF FLUIDS IN POROUS MEDIA. Amsterdam Elsevier.

BISHOP, I.D., PETTIFER, G.R., & POLAK, E.J., in prep. - Musa River hydroelectric scheme seismic survey, P.N.G., 1972. Bur. Miner. Resour. Aust. Rec. (unpubl.).

BRAYBROOKE, J.C., 1969 - Rip-rap and fill material for Mission Point Wharf, Wewak. Geol. Vulcano. Branch. Terr. PNG Dept of Lands, Surveys and Mines, Note on Invest. 69402 (unpubl.).

CARPENTER, E.G., & HABBERJAM, G.M., 1956 - A tri-potential method of resistivity prospecting. Geophysics, 21(4), 455-69.

LONDON, A.G., 1952 - Computation of permeability from simple soil tests. Geotechnique, 3, 165-83.

HABBERJAM, G.M., 1967 - On the application of the reciprocity theorem in resistivity prospecting. Geophysics 32(5), 918-9.

HABBERJAM, G.M., & WATKINS, G.E., 1967 - The reduction of lateral effects in resistivity probing. Geophys. Prosp. 15(2), 221-35.

HARRIS, J., 1971 - Groundwater for Wewak town supply. Geol. Surv. PNG Note on Invest. 71-004 (unpubl.).

TODD, D.K., 1959 - GROUNDWATER HYDROLOGY New York, Wiley & Sons.

VINCENZ, S.A., 1968 - Resistivity investigations of limestone aquifers in Jamaica. Geophysics, 33(6), 980-4.

VOZOFF, K., 1958 - Numerical resistivity analysis: horizontal layers. Geophysics, 23(3), 536-56.

WIEBENGA, W.A., & JESSON, E.E., 1962 - Geophysical exploration for underground water. Bur. Miner. Resour. Aust. Rec. 1962/72. (unpubl.).

APPENDIX 1. RESISTIVITIES OF WATER SAMPLES

Location	Resistivity (ohm-m)
Wewak Hotel bore	1.9
Mobil bore	2.9
Seeto bore	10.9
Fire station bore	13.4
Catholic Mission well	7.0
Wewak Cordials well	11.5
Sea water	0.16

APPENDIX 2. WENNER TRIPOTENTIAL METHOD

1. Introduction

This description is based largely on a paper by Habberjam & Watkins (1967). The tripotential technique was first developed to overcome some of the problems which arise with the interpretation of resistivity data. The interpretation procedures devised for resistivity depth sounding data are based on a simple layered medium model, which is rarely encountered in nature. In reality, resistivity, which is one of the most variable geophysical properties of rocks and their weathering byproducts, varies both laterally and vertically, often in a disordered manner depending on the bedding irregularities and the degree of homogeneity of the earth materials. In interpreting depth sounding data, scatter in the field data which is caused by resistivity variations other than purely vertical changes may often influence the accuracy of the layered model interpretation. The term 'lateral' is used in describing resistivity variations which are a function of horizontal distance and not of depth alone. The Wenner tripotential method, removes by a method of minimum adjustment the scatter in field data which cannot be reconciled with a purely depth variation of resistivity.

Several interpretation procedures have been devised for different electrode configurations, but, for each electrode configuration, calculations can be made from the field data of the variation of potential with distance from an isolated

current electrode. This potential-versus-distance curve is the link between all the apparently independent interpretation techniques for different electrode configurations. For the theoretical case of a horizontally layered medium the potential-distance curve must obey certain conditions. Variations from these theoretical conditions-as observed in the potential-distance curve constructed from the field data- are removed by a minimum adjustment procedure to leave a potential-distance curve which has properties complying with the layered model and which allows complete freedom of depth interpretation technique.

In practice, lateral variations arise from variations in thickness and resistivity of near surface and deep layers, lensing of beds (as in the alluvial environment) dipping layers, fissures, structural changes, and differential weathering.

2. Theory of the method

The method is based on reconstruction from the field data of the potential, ϕ, versus distance, r, curve. The field set-up for the Wenner α (CPPC) configuration is shown in Plate 19. If $\phi(r)$ is the potential at an electrode at a distance, r, from a point source of unit current entering the layered homogeneous ground, then for the Wenner configuration the resistance, $R^{\alpha}(a)$, measured at electrode spacing, a, is given by:

$$R^{\alpha}(a) = \phi(a) - \phi(2a) - \phi(2a) + \phi(a) \quad - \qquad (1)$$

whence

$$\phi(2a) = \phi(a) - R^{\alpha}(a)/2 \qquad (2)$$

For the γ configuration (CPCP, Plate 19)

$$R^{\gamma}(a) = \phi(a) - \phi(3a) - \phi(a) + \phi(a) \qquad (3)$$

Thus

$$\phi(3a) = \phi(a) - R^{\gamma}(a) \qquad (4)$$

From equation (2), if two concurrent geometric expansions of electrode spacings - say a, 2a, 4a, 8a,.....2^na, and 3a, 6a, 12a....3.2^na - are used, two separate potential distance curves can be constructed from the field $R^{\alpha}(a)$ values. Equation (4) provides the link between the two potential curves at spacings a and 3a using the field value of $R^{\gamma}(a)$ at spacing a. However several links can be defined for the field values 2a, 6a, $R^{\gamma}(2a)$ and 4a, 12a, $R^{\gamma}(4a)$ etc. In practice with field data, the links disagree because the assumption of a homogeneous layered medium is not applicable. Using the several 'links' it is possible to diagnose lateral effects and to adjust observed R^{α} and R^{γ} values to get agreement. The construction of the potential curves and the links is best illustrated by a series of ladder networks.

In Plate 19, Ladder 1 shows a series of closed loops with links, based on equations 2 and 4. The disagreements in links are manifested as misclosure around the loops and in practice misclosures can be considerable.

The theory of layered medium in resistivity states that the ϕ (r) versus r curve must obey the following conditions:-

(a) $\frac{\partial \phi}{\partial r}$ is always negative (ie potential decreases with distance from the point source)

(b) $\frac{\partial^2 \phi}{\partial r^2}$ is always positive

(c) ϕ (r) is a smooth function of r .

Any deviation from these conditions is related to lateral variations and an adjustment of the potential is carried out in three separate stages.

The first stage involves reducing the misclosures. Considering any cell in ladder 1, then if no lateral variations and hence no misclosure are present.

The following equation holds.

$$R^{\gamma}(a) - R^{\alpha}(a)/2 = R^{\gamma}(2a) - R^{\alpha}(3a)/2 \qquad (5)$$

If lateral effects and misclosures are present then:

$$R^{\gamma}(a) - R^{\alpha}(a)/2 = \left[\phi(2a) - \phi(3a)\right] + e1 \qquad (6)$$

and:

$$R^{\gamma}(2a) - R^{\alpha}(3a)/2 = \left[\phi(2a) - \phi(3a)\right] + e2 \qquad (7)$$

Putting $\Delta\phi\,(2,3) = \phi(2a) - \phi(3a)$ (8)

an estimate of $\Delta\phi(2,3)$ is obtained by averaging the two sides of equation (5):

$$\Delta\phi\,(2,3) = \tfrac{1}{2}\left\{\left[R^{\gamma}(a) + R^{\gamma}(2a)\right] - \left[\frac{R_{\alpha}(a)}{2} + \frac{R_{\alpha}(3a)}{2}\right]\right\} - \frac{(e1 + e2)}{2} \qquad (9)$$

e_1 and e_2 represent anomalous lateral effects and lacking further information on the values of e_1 and e_2 the best estimate of $\Delta\phi\,(2,3)$ is given by setting:

$$e_1 + e_2 = 0 \qquad (10)$$

If, however, one of the resistance differences - say the left-hand side of equation (5) - is negative, then it is set to zero to comply with condition (a). The ladder of resistance values (ladder of Plate 19), is formed by first setting any negative values of the resistance, differences to zero and then averaging the appropriate pair for each value of $\Delta\phi$ (2,3), etc. This gives $\Delta\phi$ (2,3), $\Delta\phi$ (4,6), $\Delta\phi$ (8,12), etc.

From ladder 1 and the resistance values, ladder 2 can be formed. By a similar arrangement to the above it can be shown that:

$$\Delta\phi\ (3,4) = \tfrac{1}{2}\left\{\left[R\frac{\alpha(2a)}{2} - \Delta\phi\ (2,3)\right] + \left[R\frac{\alpha(3a)}{2} - \Delta\phi(4,6)\right]\right\}\frac{-(e_1+e_2)}{2} \qquad (11)$$

when lateral effects are present, and by putting $\frac{1}{2}(e_1 + e_2)$ equal to zero, the best estimate of $\Delta\phi$ (3,4) is obtained. Again if either of the terms in the square brackets are negative, then to comply with condition (a) they are set to zero and then finally averaged. Ladder 3 is formed from the two ladder adjustments. Condition (a) is then satisfied and potential is a decreasing function of distance. $R\alpha(a)/2$ gives a single estimate of $\Delta\phi$ (1,2). For the second stage the chord slopes must be adjusted.

Condition (b) requires that the chord slopes $\Delta\phi$ (2,3)/a, $\Delta\phi$(3,4)/a, $\Delta\phi$(4,6)/2a, etc, are decreasing.

$$\text{i.e. } \frac{\Delta\phi(2,3)}{a} > \frac{\Delta\phi\ (3,4)}{a} > \frac{\Delta\phi\ (4,6)}{2a} \qquad \text{etc.}$$

If any two successive chord slopes do not obey this condition they are made equal by replacing them both with a chord slope equal to the total of the two potential differences involved, divided by the combined spacing. For example, if $\frac{\Delta\phi(2,3)}{a} < \frac{\Delta\phi(3,4)}{a}$, then they are both replaced by $\left[\Delta\phi\ (2,3) + \Delta\phi\ (3,4)\right] / (a+a)$. This process can be extended to three or more successive slope differences if necessary.

The third stage requires smoothing of the potential-distance data to satisfy the less rigorous condition (c), a local smoothing technique is used. A potential curve is constructed from the adjusted potential differences, and the $r \cdot \phi(r)$ curve is smoothed. Plate 19 shows the smoothing technique used. The final, $\phi_s(r)$ (smoothed potential) values

are used to recalculate the smoothed Wenner resistances (see equation (2)) and from these, resistivities can also be calculated. Alternatively the smoothed potential curve can be used for direct methods of interpretation. Schlumberger curves can be constructed from values of $\delta\phi/\delta r$ calculated from the smoothed potential curve using Lagrangian interpolation. Thus, complete flexibility of interpretation is available; however, for the purposes of the current interpretation, the smoothed Wenner curves were used to derive resistivity layered models.

3. Lateral Inhomogeneities Index (LII)

In ladders 1 and 2 (plate 19), non-closure of the loops of the ladders are represented by ($e1 - e2$); putting ($e1 - e2$) equal to C_{23} and using the approximation that $e_1 + e_2 = 0$, then the misclosure C_{23} is made up of two equal and opposite parts.

A Lateral Inhomogeneity Ratio (LIR) is defined as the ratio of the part of the potential difference which can be assigned to lateral changes, to the final smoothed (layered model) potential difference. This can be written as $C_{23/2}\Delta\phi_s$ (2,3). This value applies only to a single cell of the first ladder; however, ratios can be derived for each cell in ladders 1 and 2. The LIR values form a continuous series.

$$C_{23/2}\,\phi_s\,(2,3),\quad C_{34/2}\,\phi_s(3,4),\quad C_{46/2}\,\phi\,(4,6)\,..\,C_{nq/2}\,\phi_s\,(n,q)$$

The Lateral Inhomogeneity Index is defined as:

$$\text{LII}\ \left\{\frac{1}{m}\sum_{m}\left(C_{nq/2}\Delta\phi_s\ (n,q)\right)^2\right\}^{\frac{1}{2}}$$

and represents an average measure of lateral influences for the whole depth probe. LII values less than 0.2 and are considered low; between 0.2 to 0.5, moderate; and high LII values are greater than 0.5.

APPENDIX 3

FIELD TESTS OF THE WENNER TRIPOTENTIAL METHOD

The tripotential method was tested in a beach environment at Moruya Heads, NSW. Depth soundings were carried out at the high-tide mark (HWM) and 15 m above the HWM. The area was chosen to simulate conditions encountered in the Wewak

area, where resistivity decreases at depth owing to the presence of salt water. In the field tests, alpha, beta and gamma readings were taken. The readings were taken using a Hewlett Packard power supply as a transmitter and a BMR constructed spontaneous potential backoff device and a Data Precision digital multimeter as a receiver.

The results are presented in Plate 20. Moruya 1 (at 15 m above the HWM) shows scatter in the results owing to poor electrode contact in the dry sand, whereas data for the depth probe Moruya 2 (at the HWM) is smoother because of the damp sand in this area.

Both depth probes show high LII values. Interpretation of the field alpha soundings reveales essentially three-layer interpretations. The smoothed curves indicate four layers. For the sounding at the HWM, an 8-ohm-m layer is introduced beneath the 24-ohm-m surface layer. The surface layer shows high lateral variation in resistivity (16-48 ohm-m) as shown by the different asymptotes at low electrode spacings. In particular the gamma and alpha soundings show high incompatibility at lower electrode spacings. Adjusting the differences between these two curves has introduced a fourth layer.

Moruya 2 (at the HWM) shows scatter, particularly at larger electrode spacings, and the adjustment has introduced a higher-resistivity layer beneath the second layer.

Further tests using the method with a more powerful resistivity transmitter in alluvial environments around Canberra suggest greater reliability of data if resistances are calculated from measured received voltages and transmitted currents. Reading errors can be kept to better than 1 percent by this method. For this reason the meggar instrument used on the Wewak survey is considered on hindsight to be not ideally suited to tripotential measurements.

The computer reduction program used has been tested against a computer program used by Dr Habberjam, University of Leeds, UK, and the programs give identical smoothed sounding curves. Habberjam (pers. comm.) suggests that, for Moruya 2, sounding the introduction of an intermediate layer is a direct result of the incompatibility of the alpha and gamma curves. Habberjam, in considering Wewak 14 sounding, suggested data errors may be more significant factor in producing an apparent deepening on the smoothed sounding curve. Habberjam suggests that it is difficult to envisage any reason why this should occur consistently, unless highly anisotropic layers are present, which is unlikely in alluvial environments such as Wewak. The important point, however, is that the high LII values render any layered interpretation unreliable.

APPENDIX 4

SEISMIC SURVEY OF THE PROPOSED NAGAM RIVER BRIDGE SITE

At the request of the Public Works Department three seismic spreads (2-m geophone spacing) were completed on the banks of the Nagam River at the proposed location of a high-level bridge to replace the existing low-level crossing. All spreads were limited in length by the terrain. The results of the seismic work and a traverse plan are given in Plate 21.

The highest seismic velocity detected (1600 m/s) is interpreted as weathered mudstone. This weathered mudstone is overlain by 4 to 6 m of soil and clay (300-500 m/s). Layering is uniform on the Maprik side of the river, but, on the Wewak side, bedrock dips as illustrated in section AB (Plate 21).

We believe that the 1600 m/s material would form a suitable foundation for the proposed bridge.

PLATE I

GEOLOGY OF WEWAK, AND LOCATIONS OF DEPTH PROBES

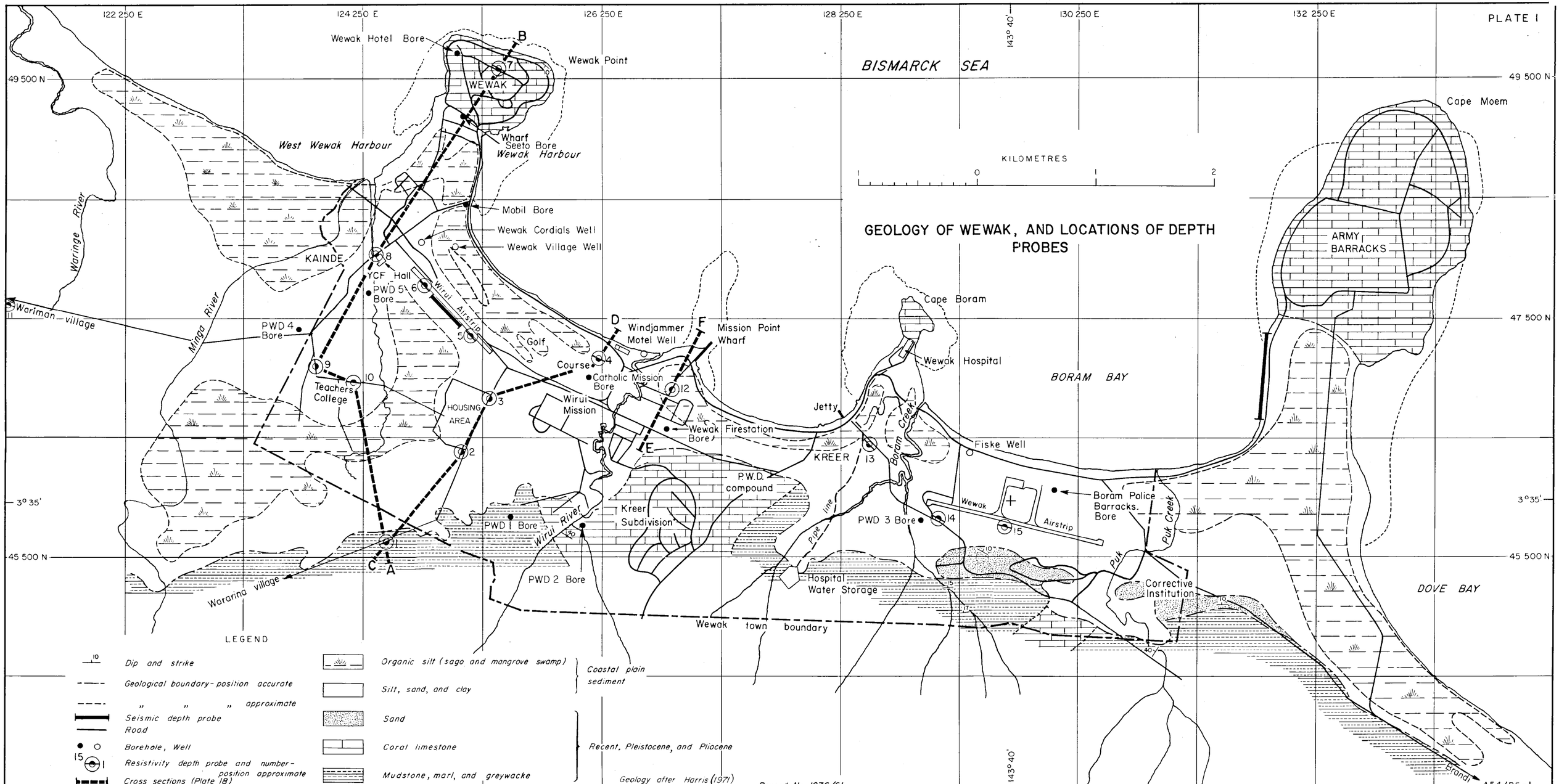

LEGEND

- Dip and strike
- Geological boundary - position accurate
- " " " approximate
- Seismic depth probe
- Road
- Borehole, Well
- Resistivity depth probe and number - position approximate
- Cross sections (Plate 18)

- Organic silt (sago and mangrove swamp)
- Silt, sand, and clay
- Sand
- Coral limestone
- Mudstone, marl, and greywacke

Coastal plain sediment

Recent, Pleistocene, and Pliocene

Geology after Harris (1971)

Record No. 1976/61

PLATE 2

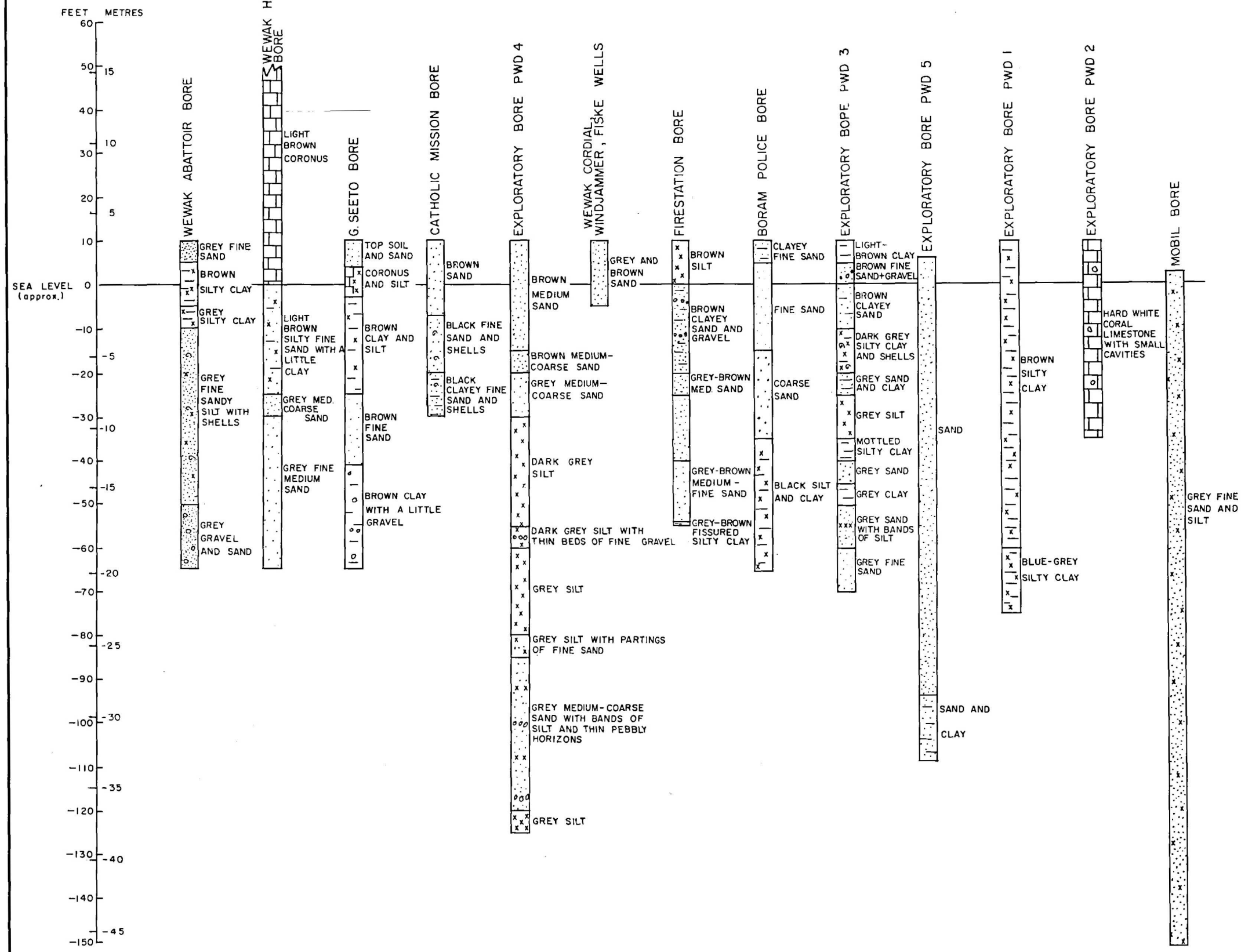

DIAGRAMMATIC GEOLOGICAL LOGS OF BOREHOLES AND WELLS, WEWAK AREA (after Harris, 1971)

Record No. 1976/61

A54/B5-2

PLATE 3

DP. No. 1 Wewak PNG

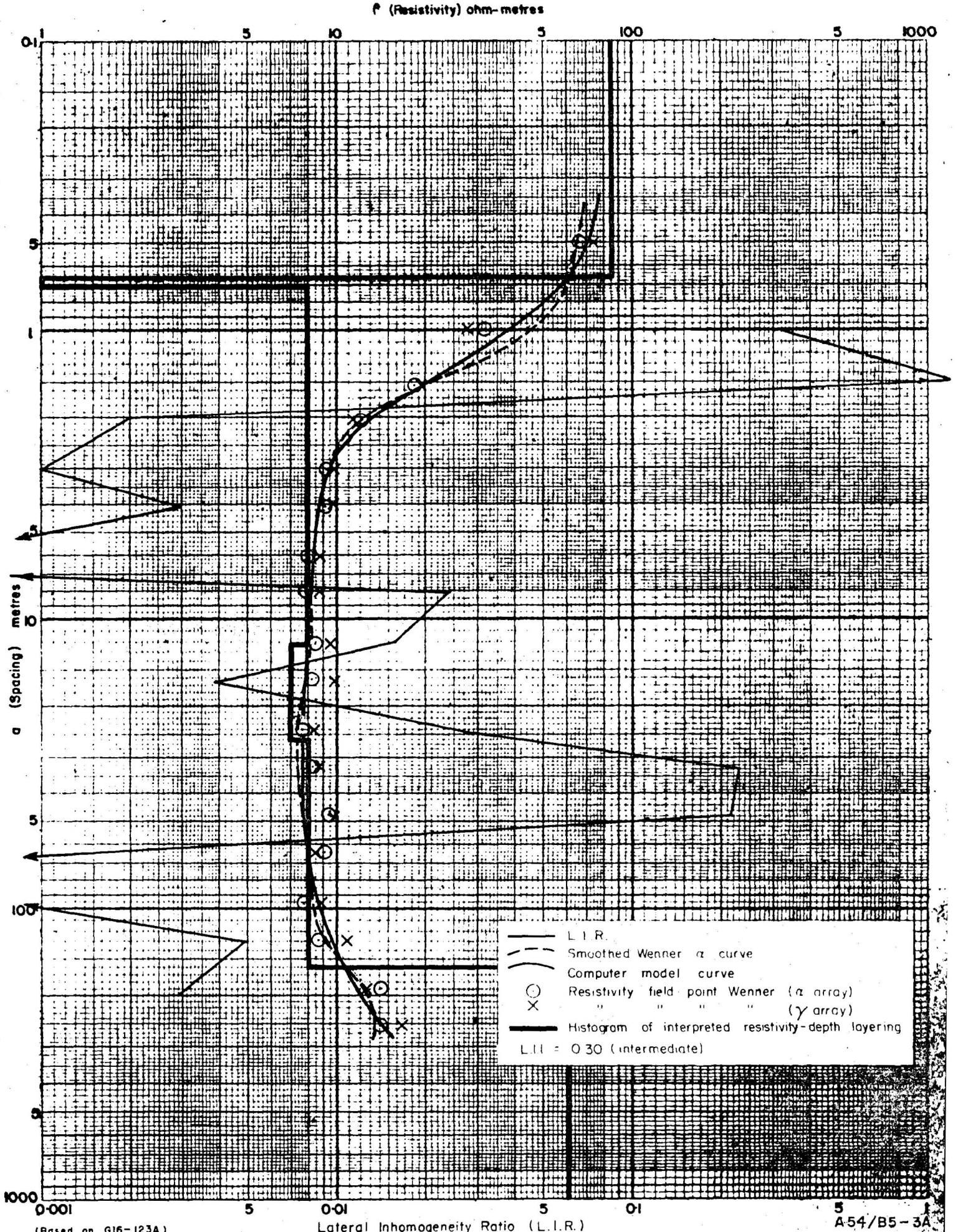

(Based on G16-123A)

A-54/B5-3A

Record No. 1976/61

DP. No. 2 Wewak PNG

PLATE 4

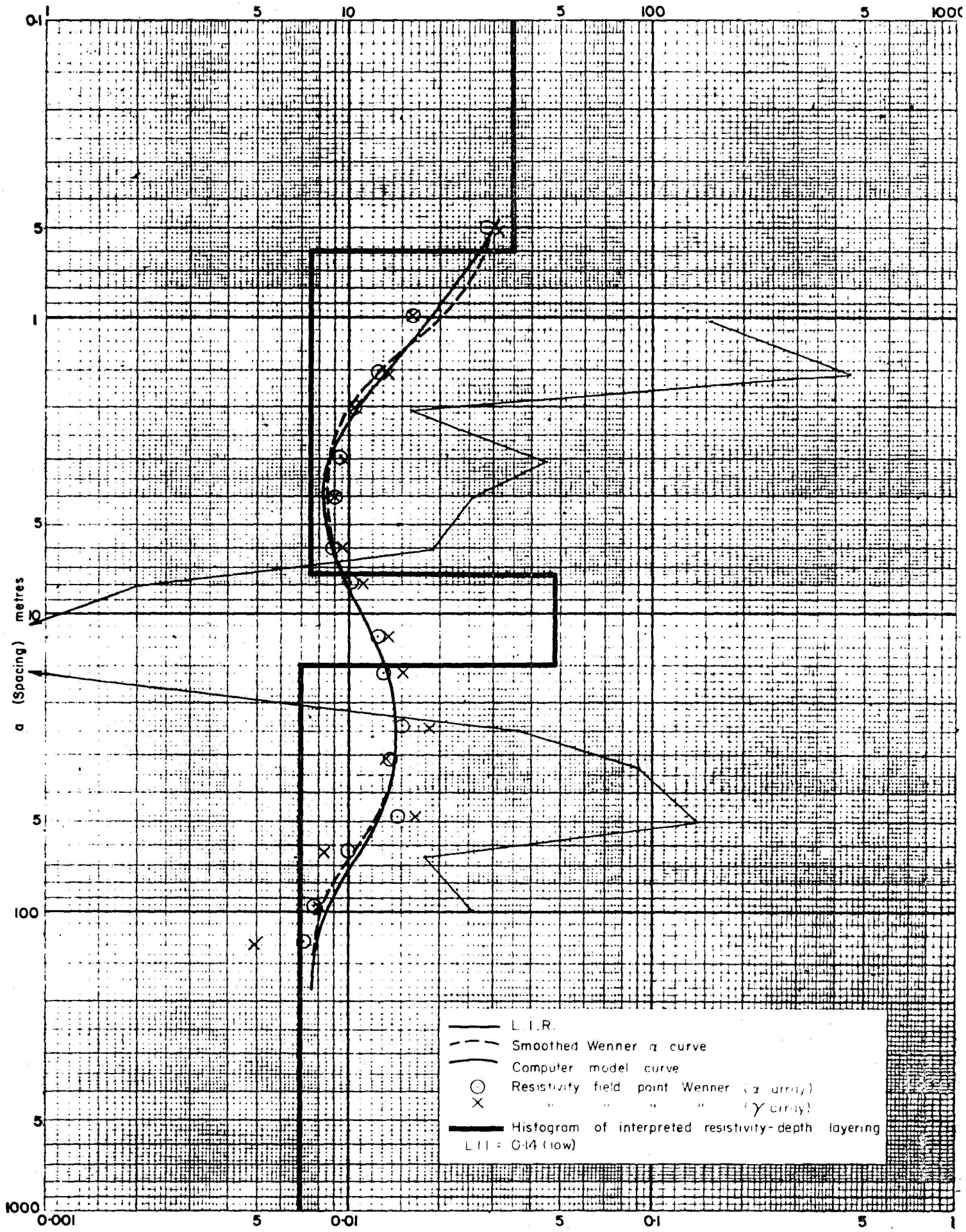

(Based on G16-123A)

A54/B5-4A

Record No. 1976/61

DP. No. 3 Wewak PNG

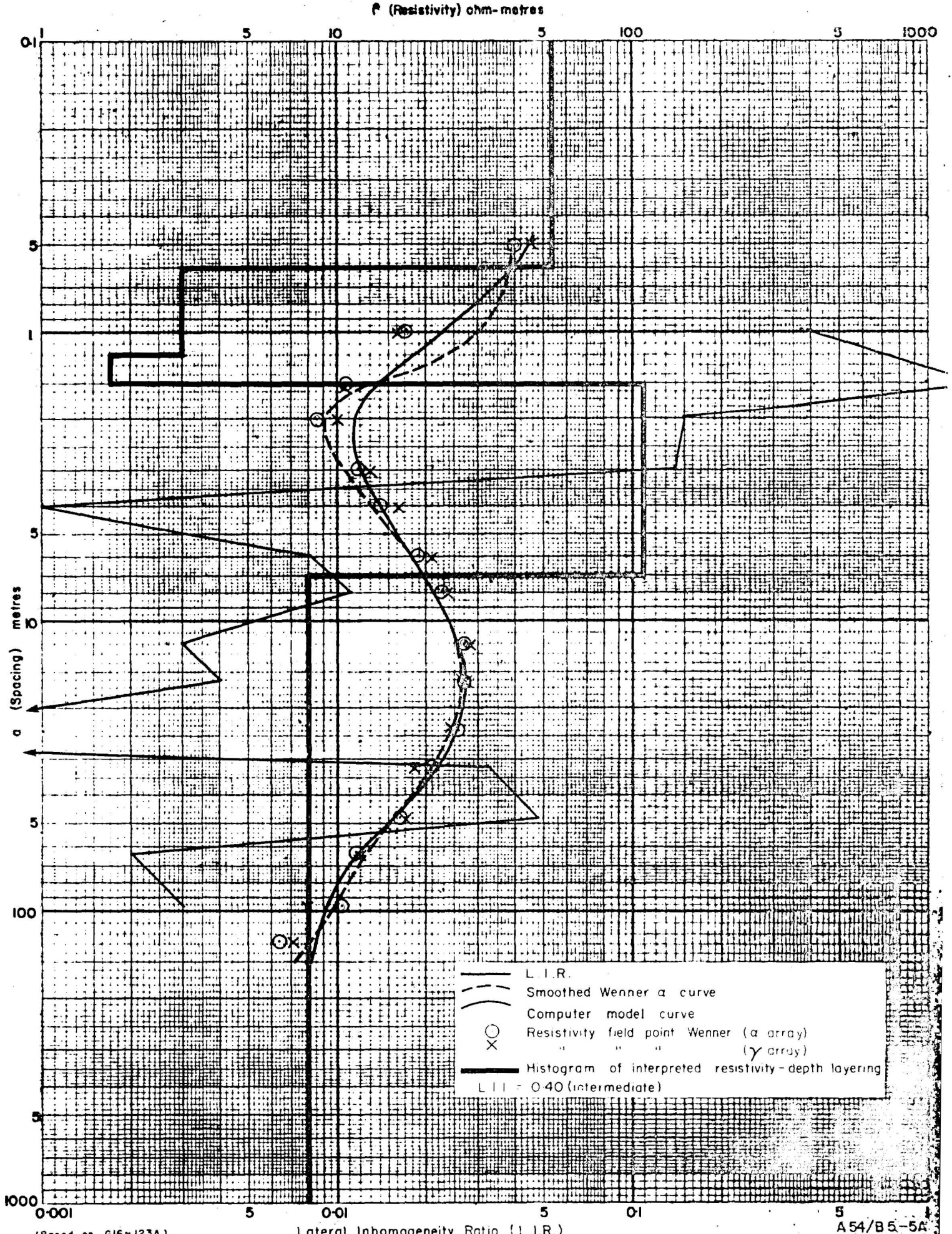

(Based on G16-123A)

Record No. 1976/61

A54/B5-5A

DP. No. 4 Wewak PNG

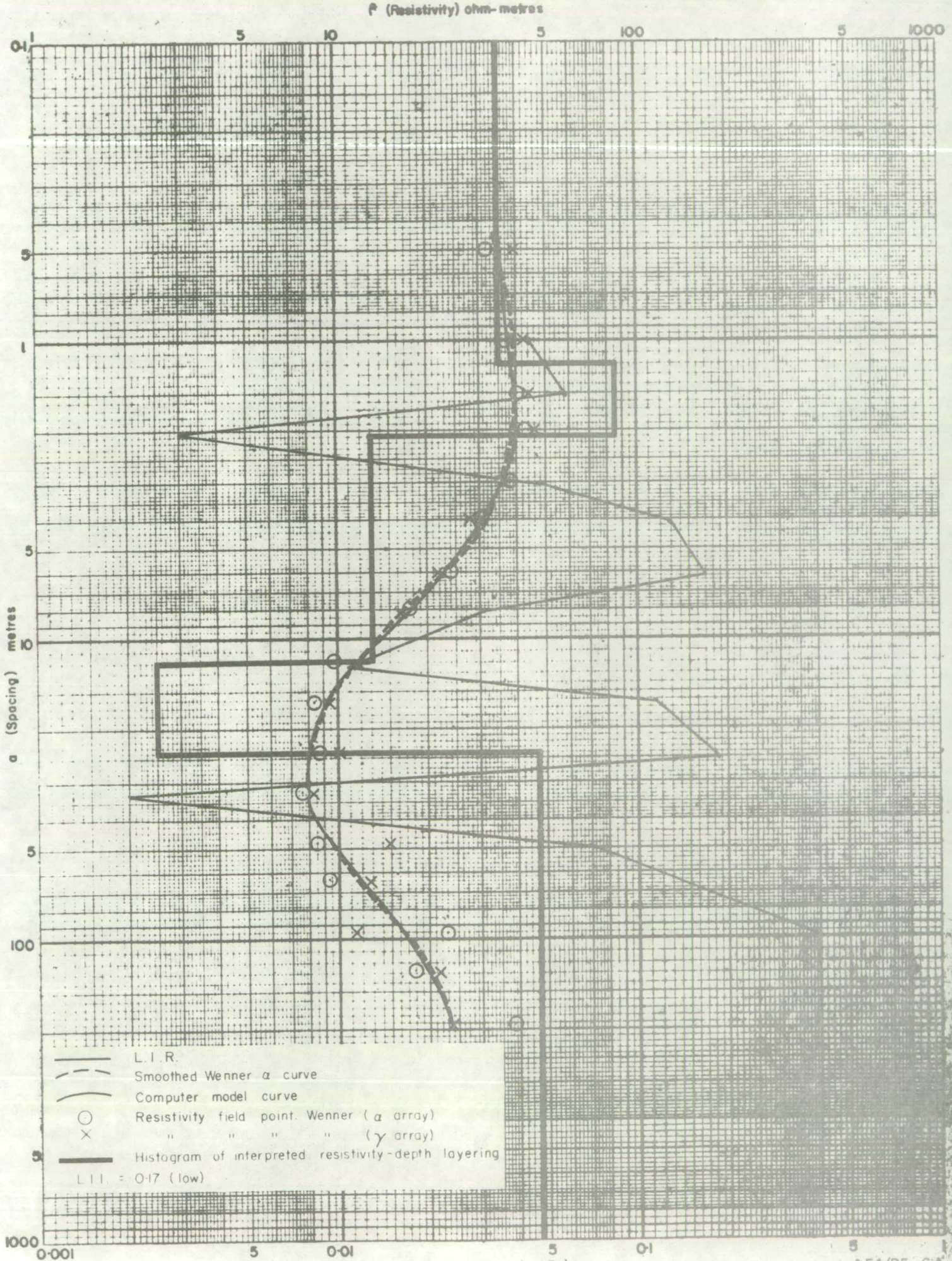

(Based on G16-123A)

Record No. 1976/61

A54/B5-6A

PLATE 7

DP. No. 5 Wewak PNG

ρ (Resistivity) ohm-metres

0·1 0 1 1 5 10 5 100 5 1000

a (Spacing) metres

0·1 5 1 5 10 5 100 5 1000

0·0001 0·001 5 0·01 5 0·1 5 1

Lateral Inhomogeneity Ratio (L.I.R.)

Based on G16-123A)

L.I.R.
Smoothed Wenner α curve
Computer model curve
⊙ Resistivity field point Wenner (α array)
× " " " " (γ array)
Histogram of interpreted resistivity-depth layering
L.I.I. = 0·59 (high)

Record No. 1976/61

A54/85-7

PLATE 8

DP. No. 6 Wewak PNG

ρ (Resistivity) ohm-metres

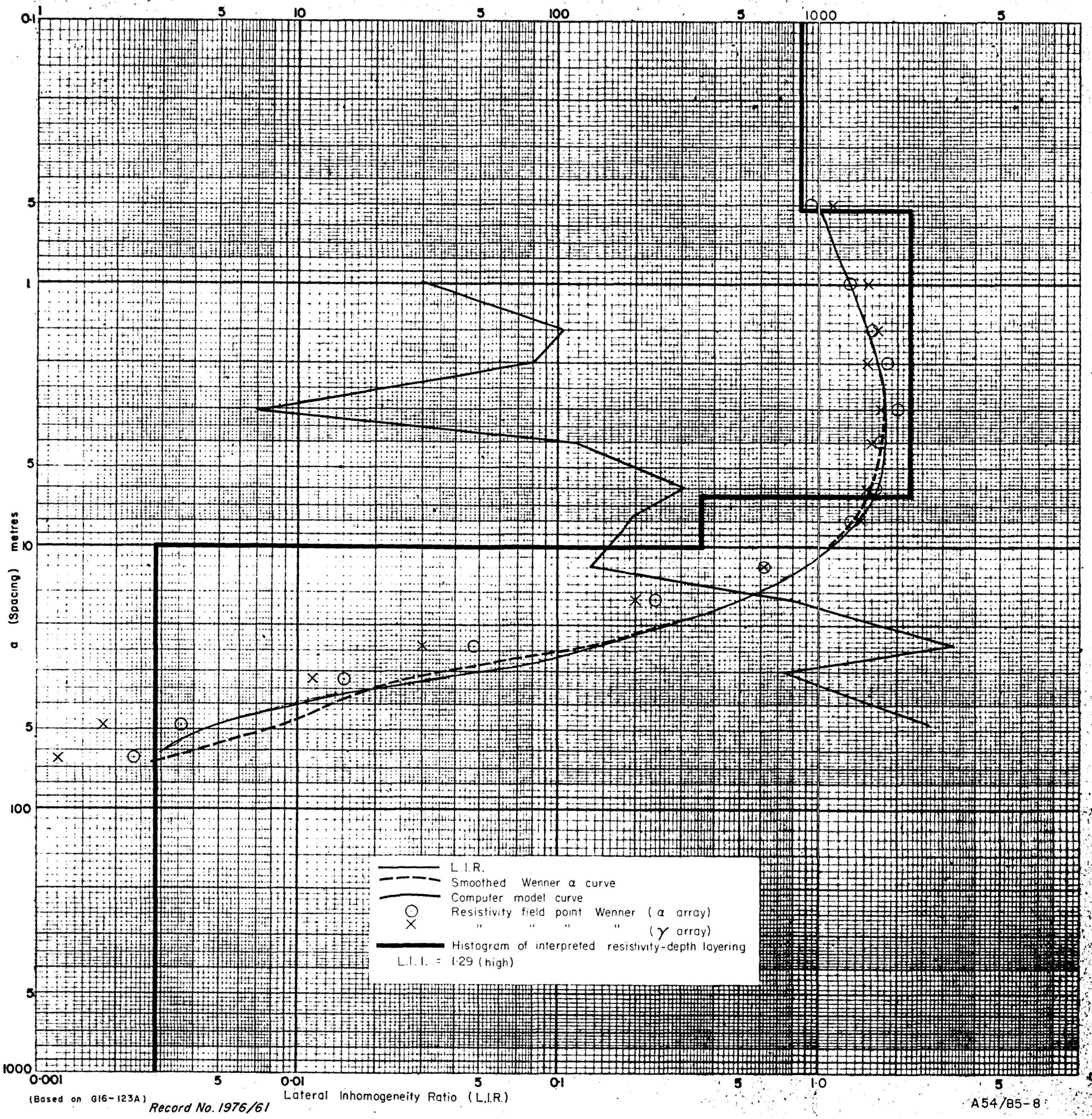

(Based on G16-123A)

Record No. 1976/61

A54/B5-8

PLATE 9

DP. No. 7 Wewak PNG

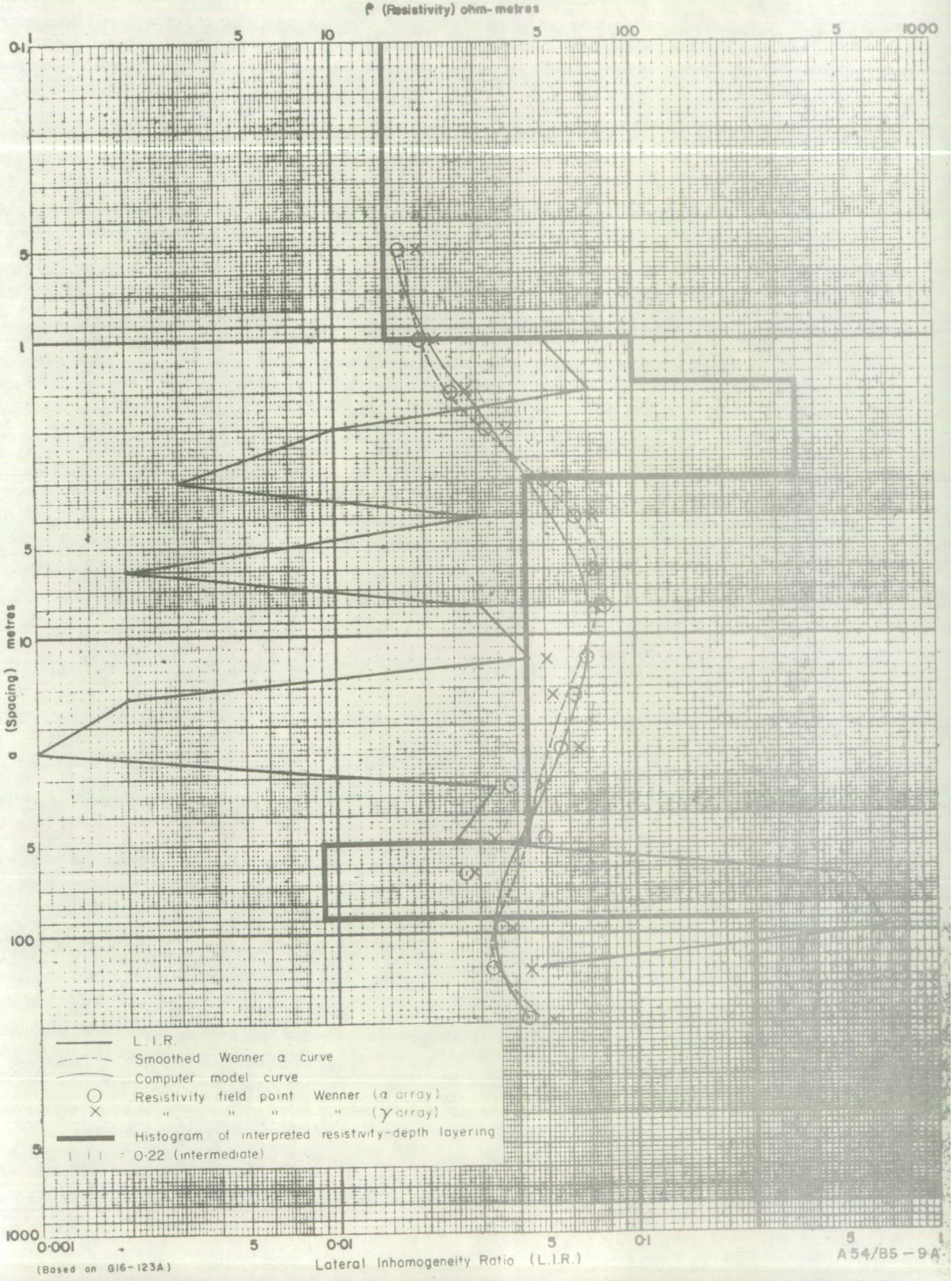

(Based on G16-123A)

A54/B5-9A

Record No. 1976/61

PLATE 10

DP. No. 8 Wewak PNG

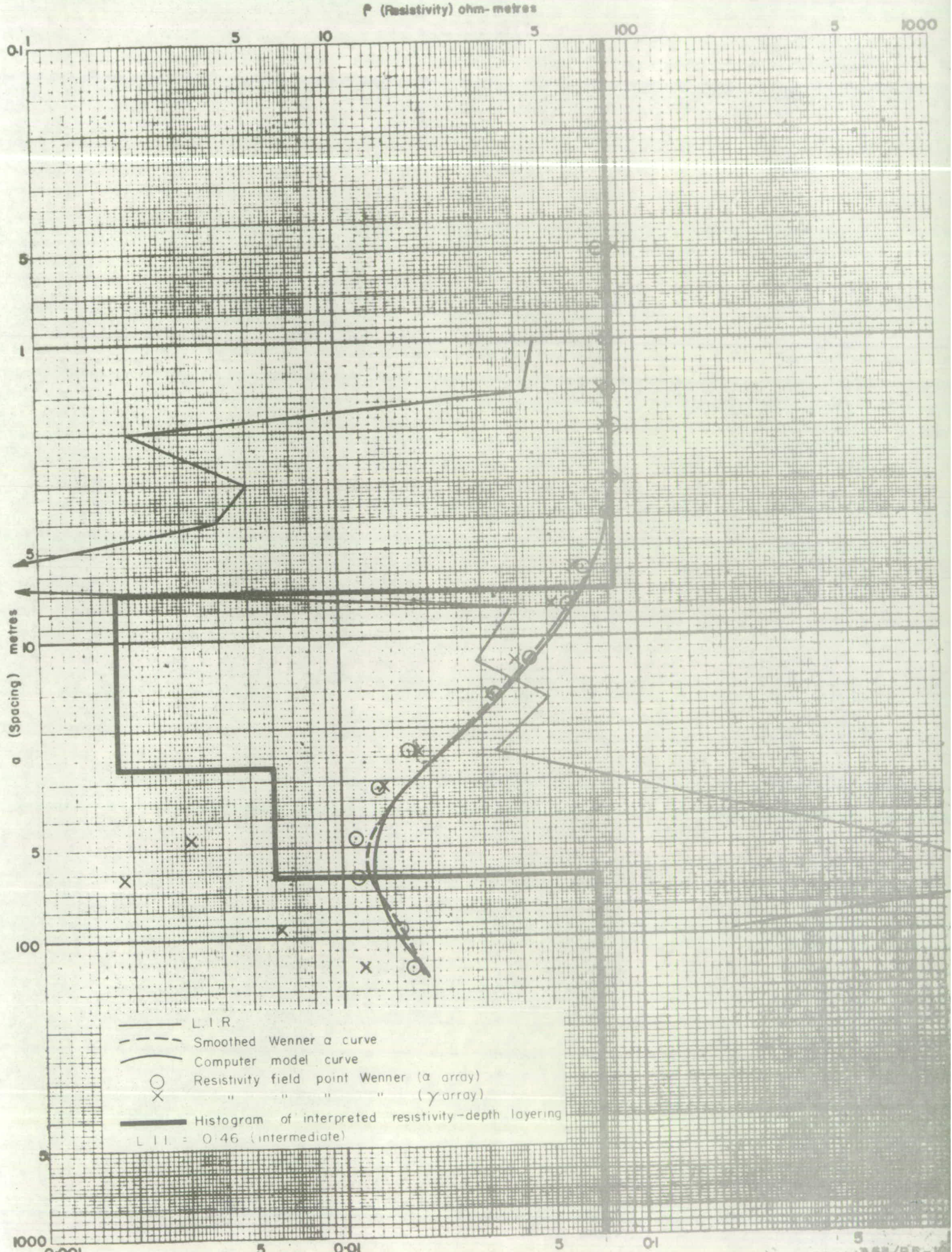

(Based on G16-123A)

Record No. 1976/61

ASR/BD-10

PLATE II

DP. No. 9 Wewak PNG

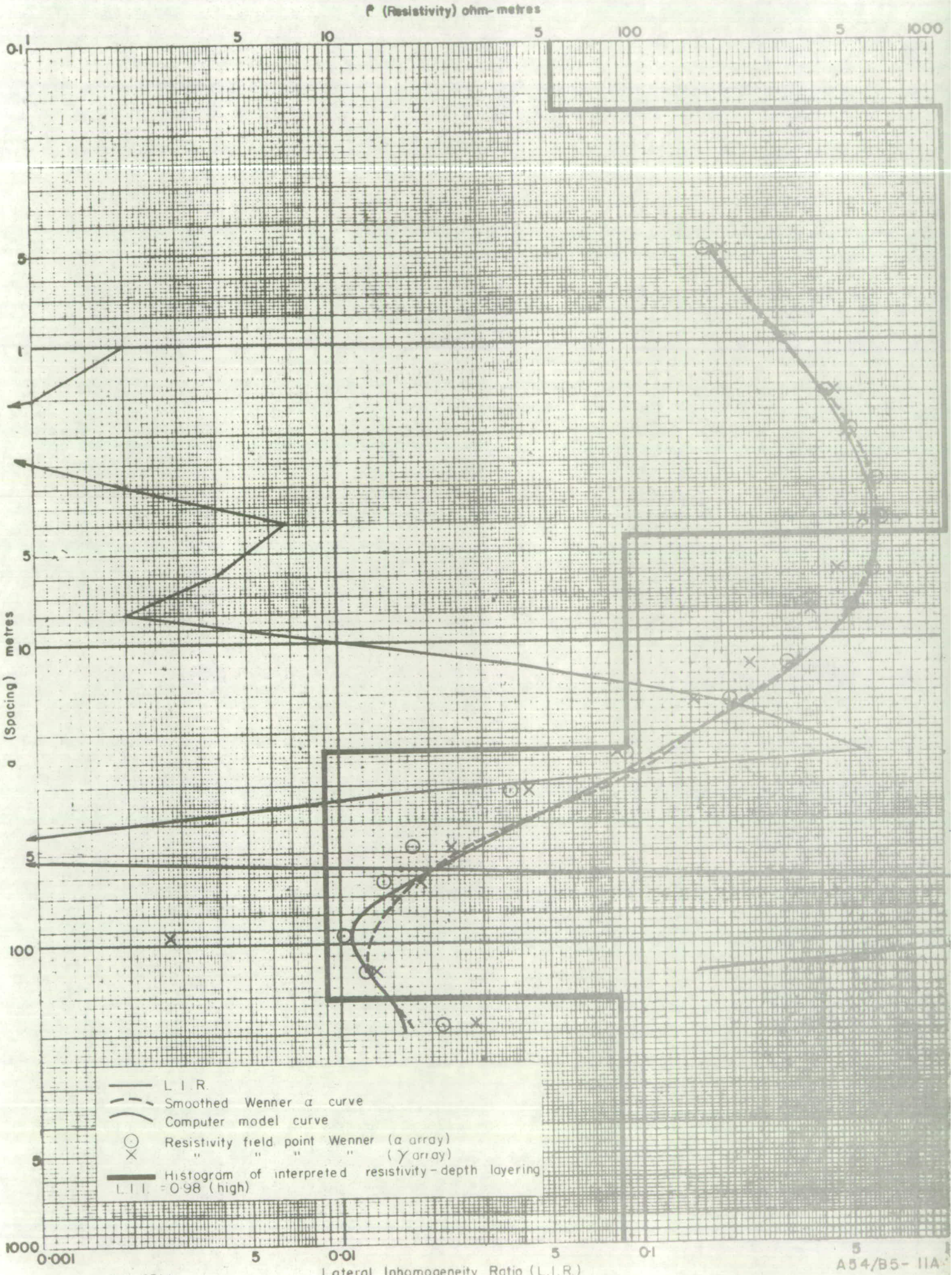

(Based on G16-123A)

A54/B5-IIA

Record No. 1976/61

PLATE 12

DP. No. 10 Wewak PNG

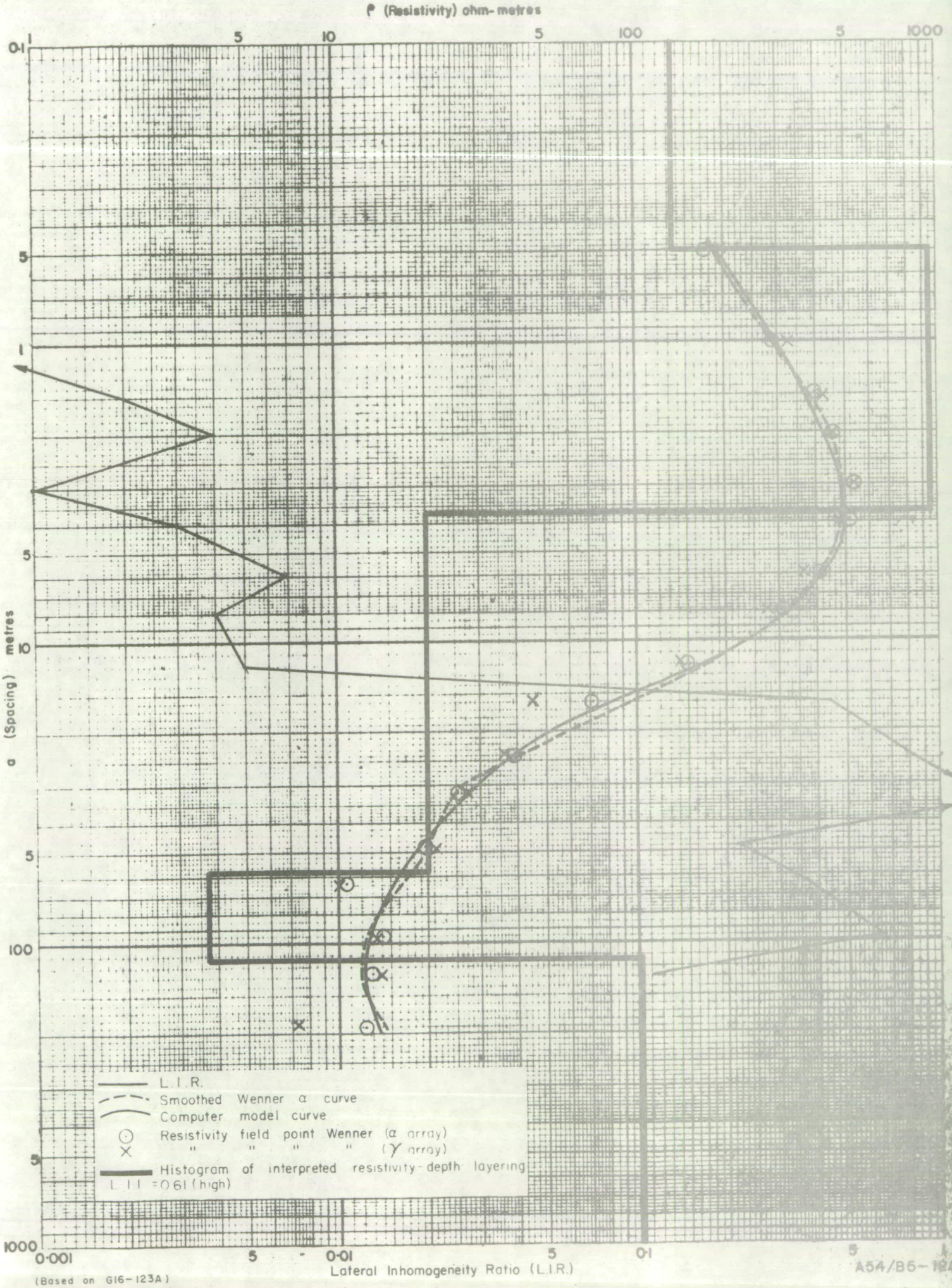

(Based on G16-123A)

Record No. 1976/61

A54/B6-12A

PLATE 13

DP. No. 11 Wewak PNG

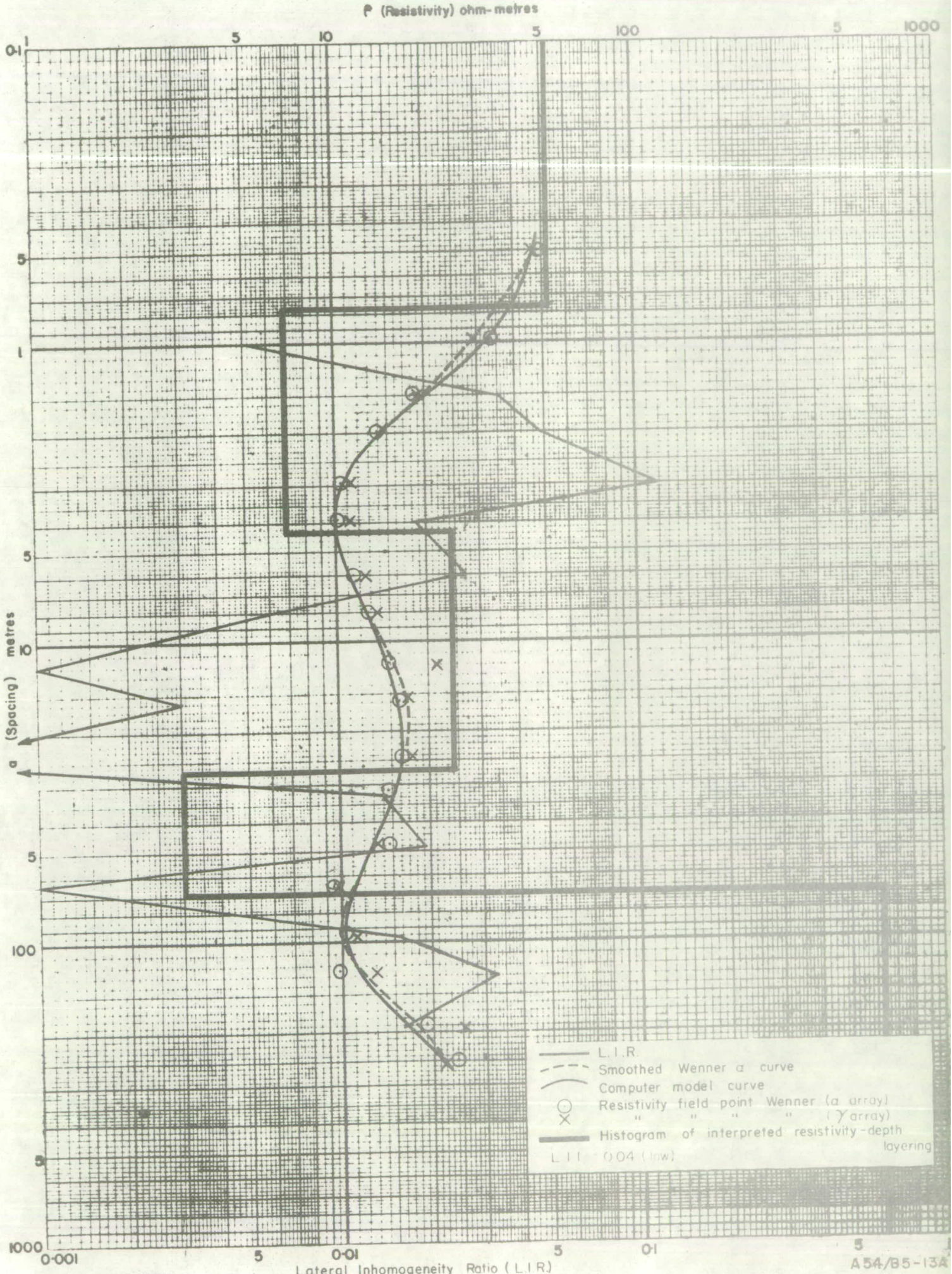

(Based on G16-123A)

Record No. 1976/61

A54/B5-13A

PLATE 14

DP. No. 12 Wewak PNG

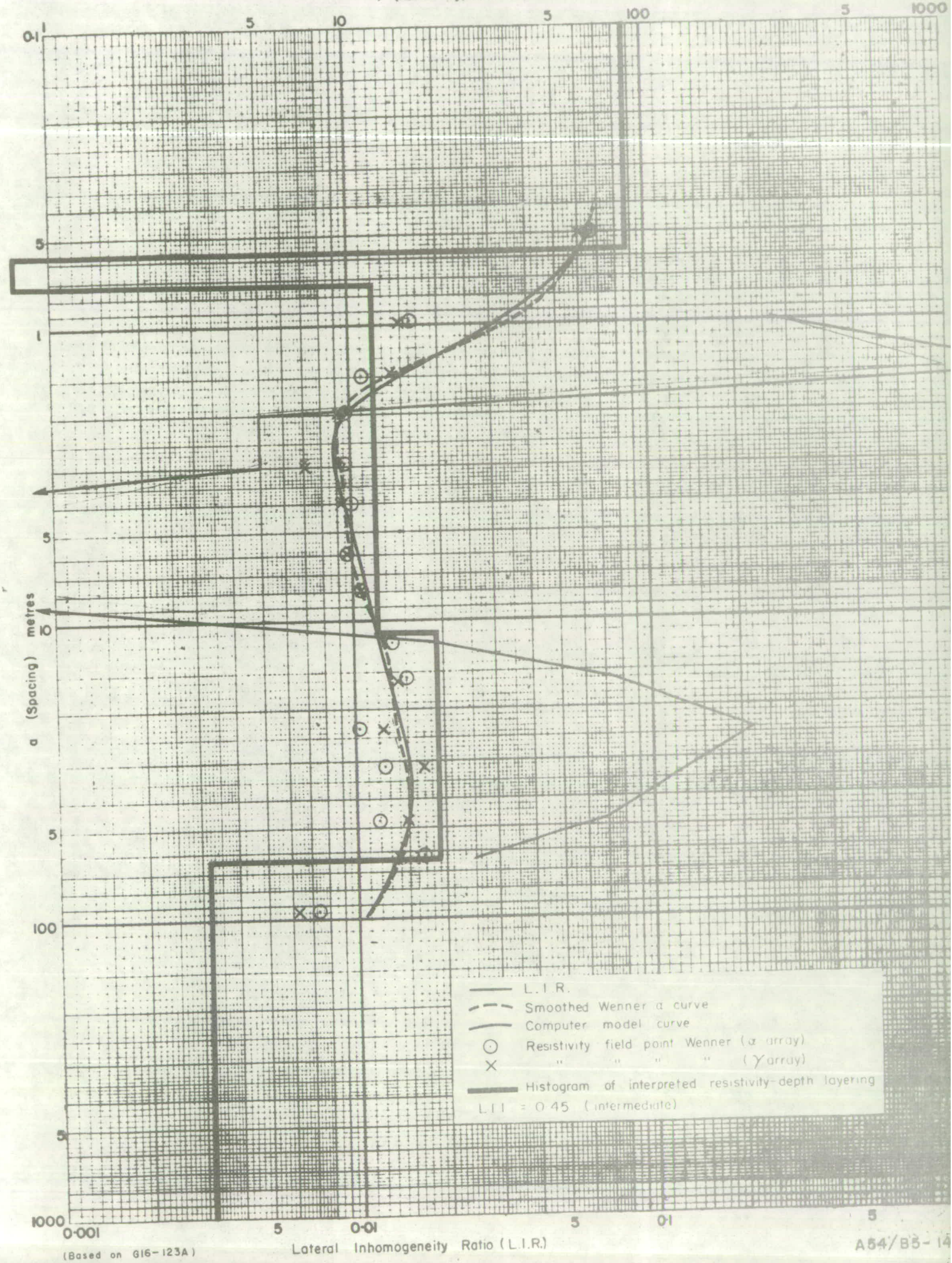

(Based on G16-123A)

Record No. 1976/61

A54/B5-14

PLATE 15

DP. No. 13 Wewak PNG

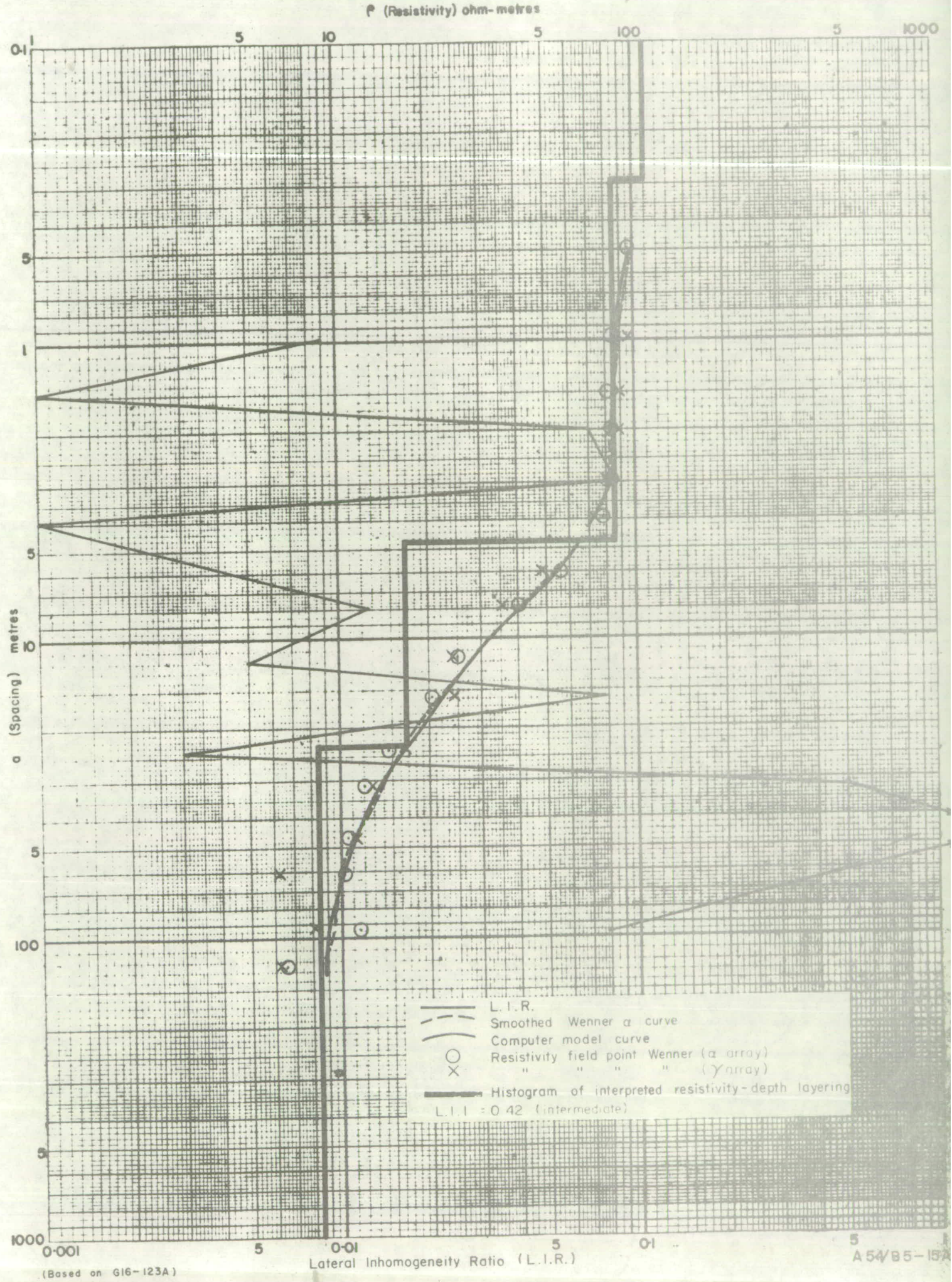

(Based on G16-123A)

Record No. 1976/61

A54/B5-15

PLATE 16

DP. No. 14 Wewak PNG

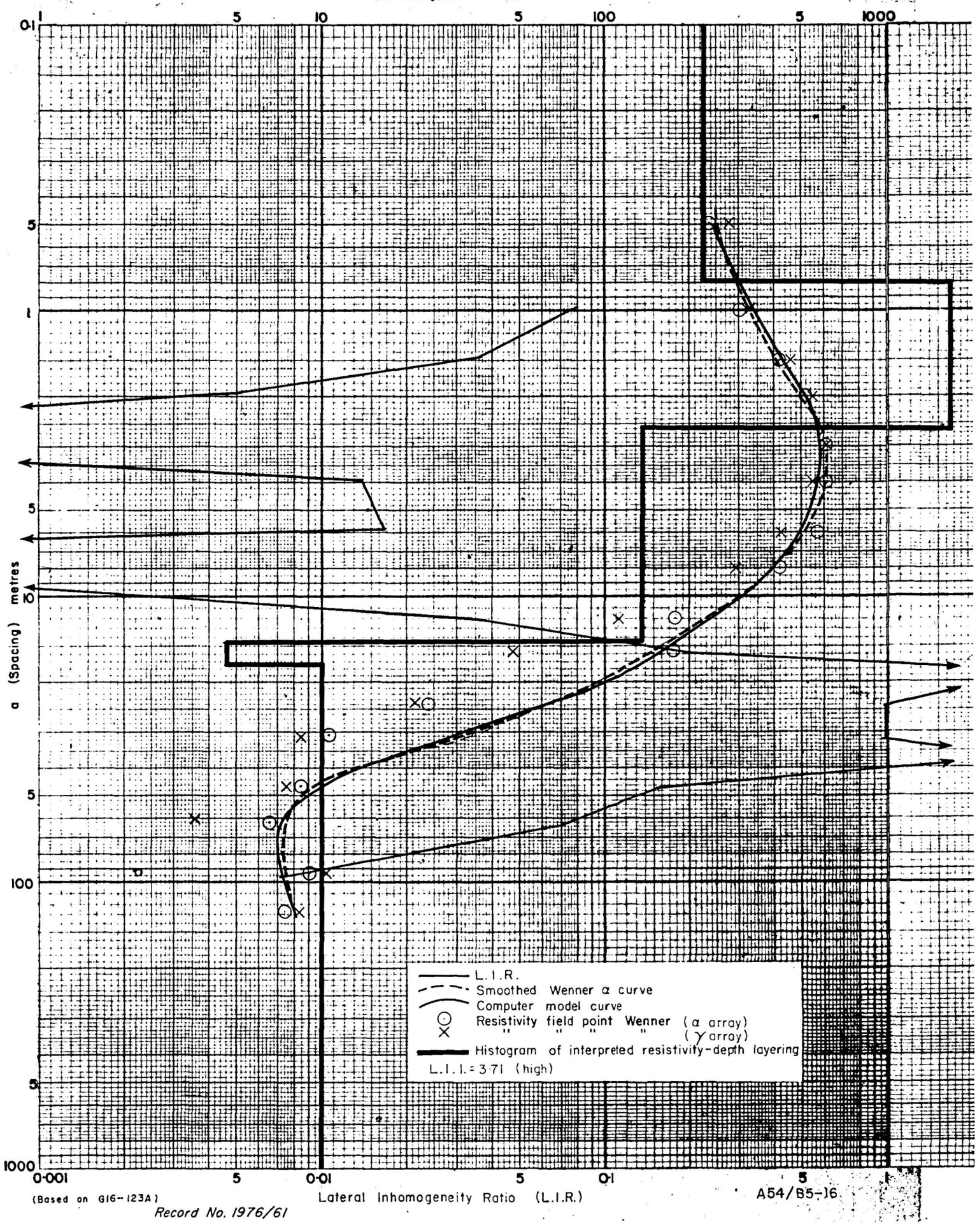

(Based on G16-123A)

A54/B5-16

Record No. 1976/61

DP. No. 15 Wewak PNG

ρ (Resistivity) ohm-metres

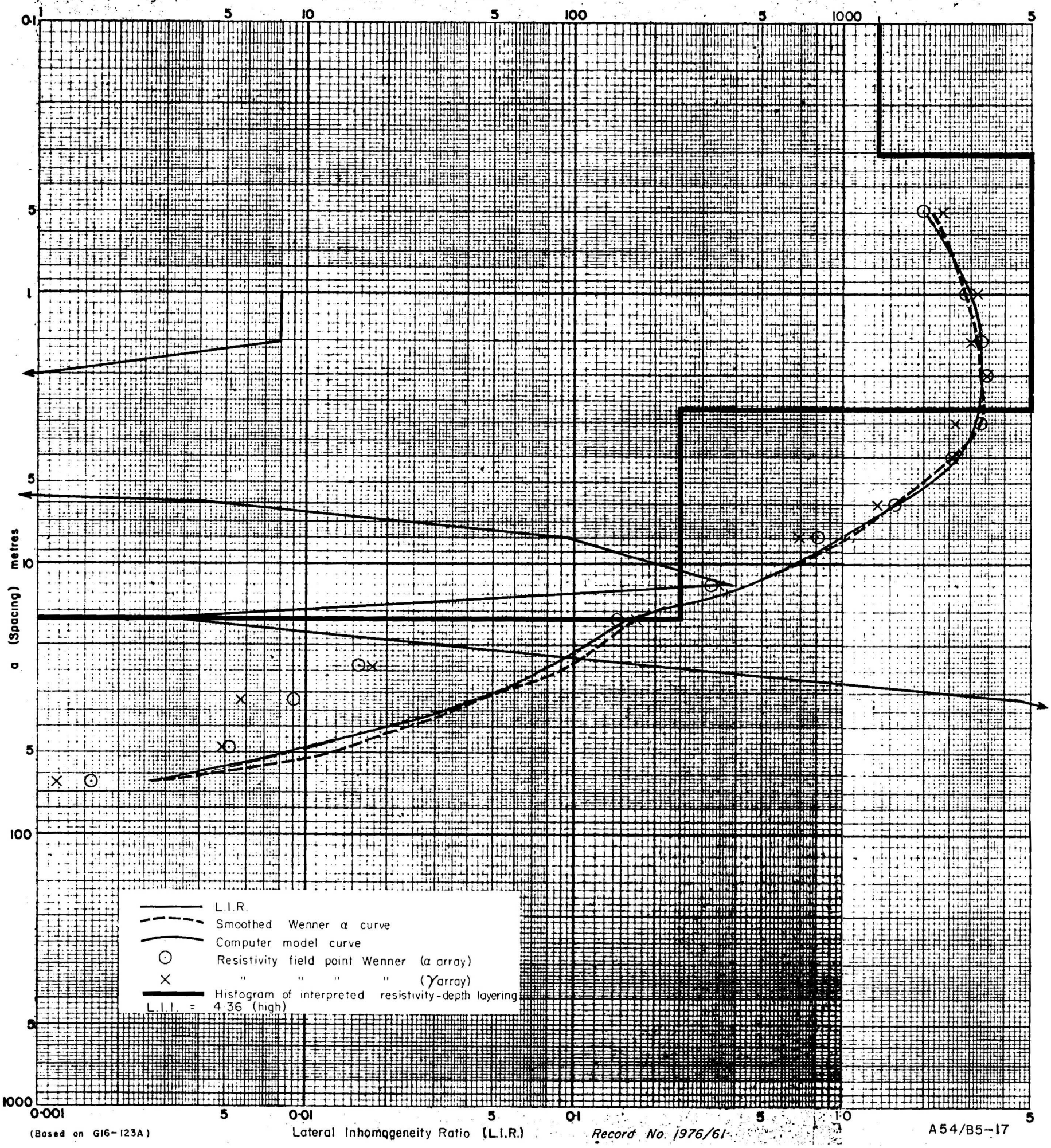

Record No. 1976/61

A54/B5-17

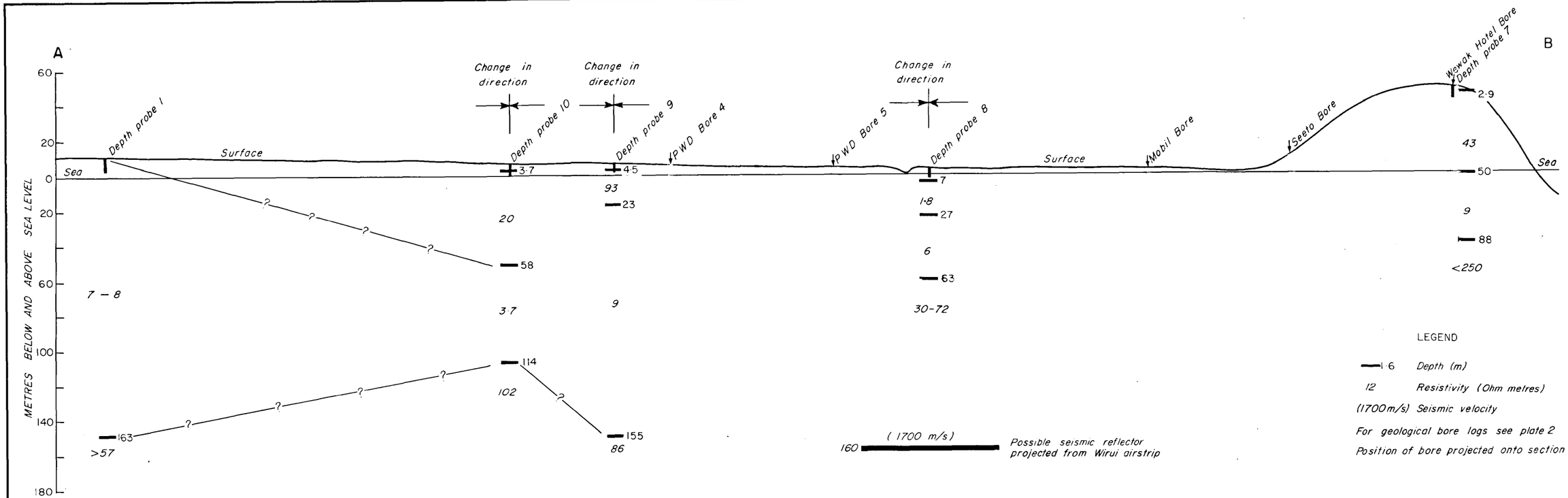

SCHEMATIC CROSS-SECTIONS OF THE COASTAL PLAIN SEDIMENTS

Record No. 1976/61

FIELD CONFIGURATIONS

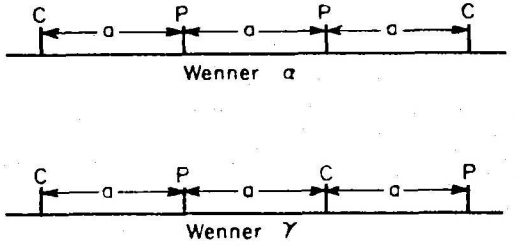

SMOOTHING TECHNIQUE

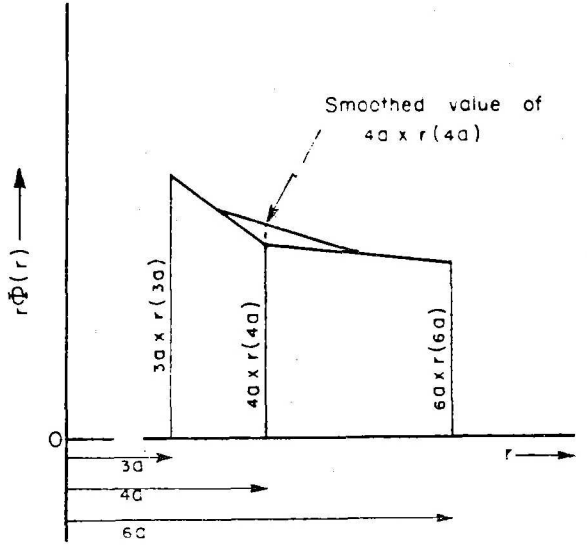

LADDER ADJUSTMENT METHOD

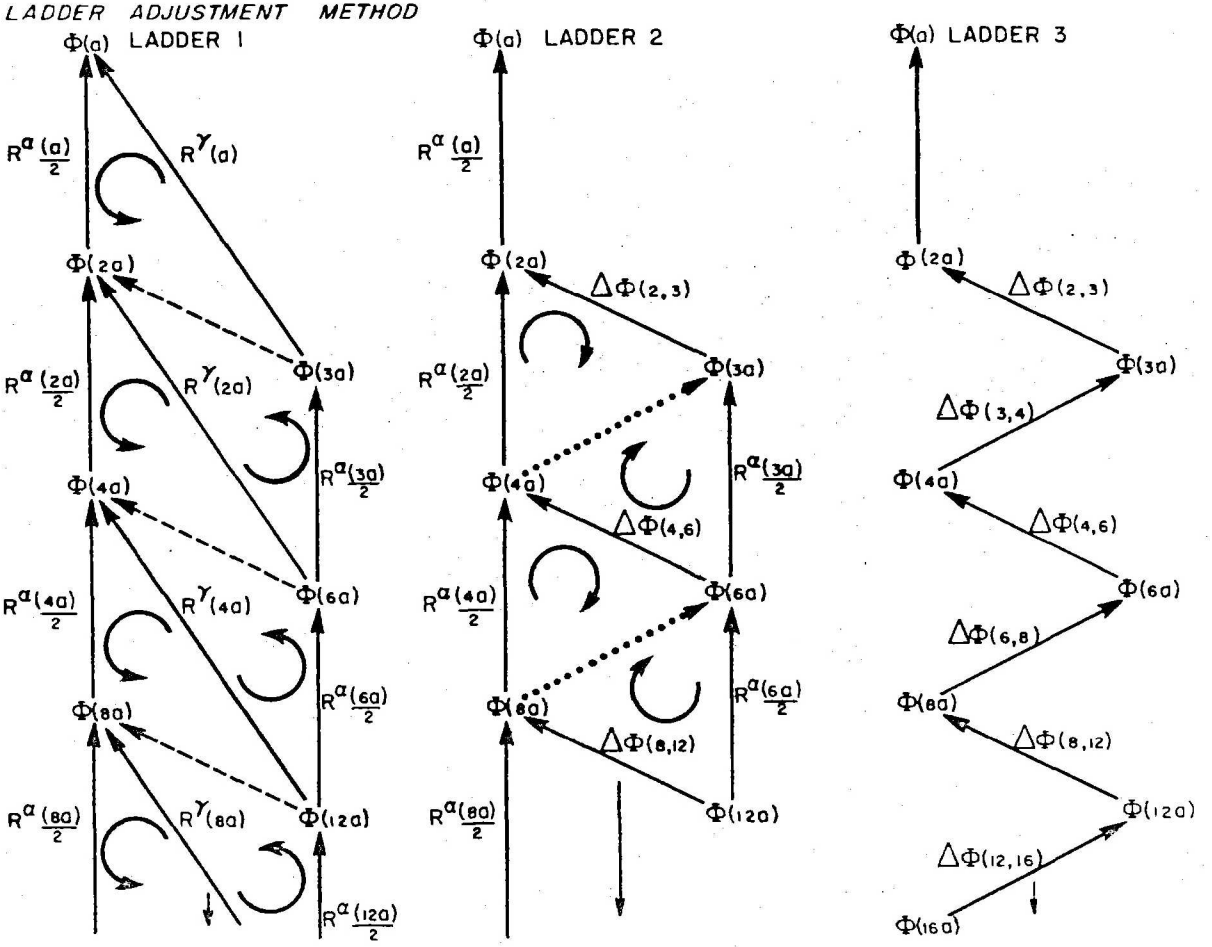

Ladder 1 : Observed resistance values link potentials shown if lateral effects are absent. Dashed lines indicate first potential difference to be derived

Ladder 2 : Second potential differences (dotted line) are derived from the combination of $R^{\alpha}/2$ *and* $\Delta\Phi$ *values*

Ladder 3 : Succession of potential differences (before ordering).

WENNER TRIPOTENTIAL METHOD
(after Habberjam & Watkins, 1967)

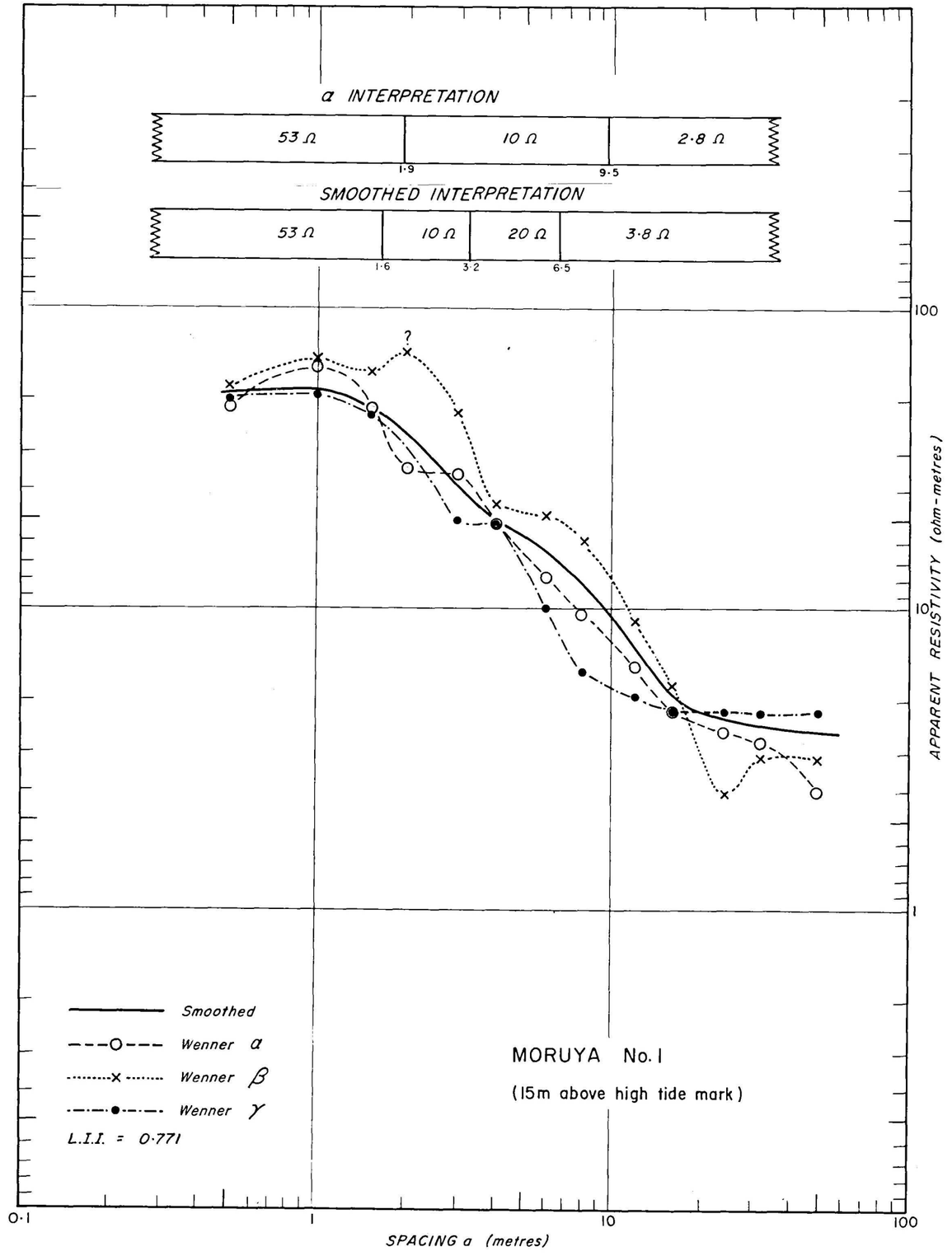

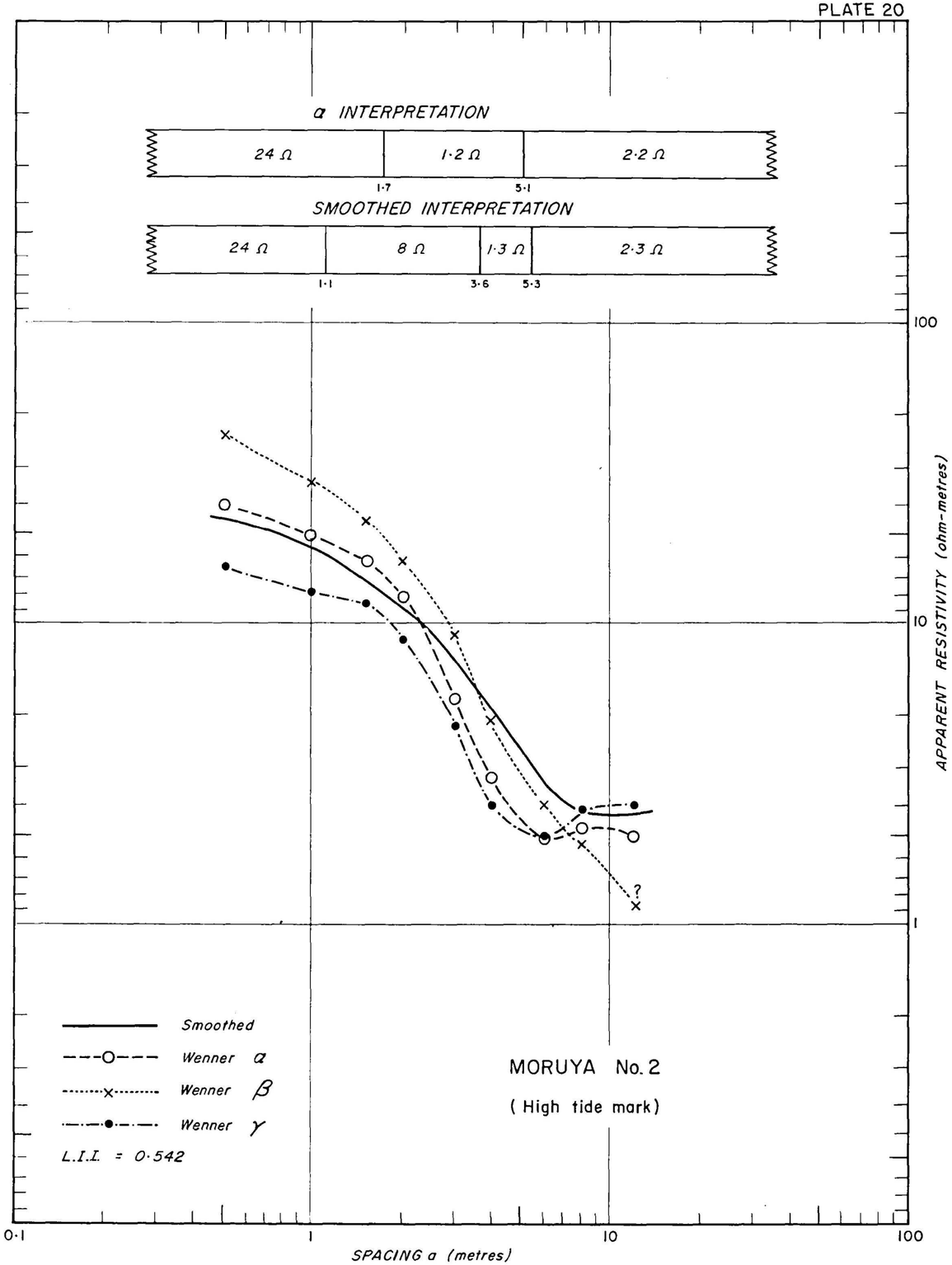

I56/B5-33

Record No. 1976/61

FIELD TESTS OF WENNER TRIPOTENTIAL METHOD—MORUYA, NSW

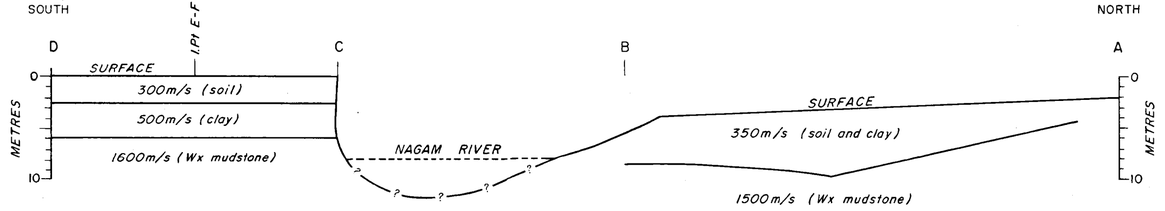

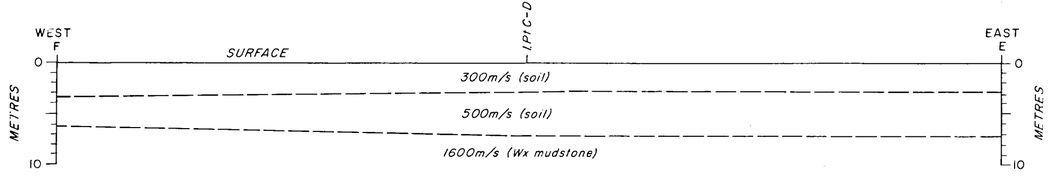

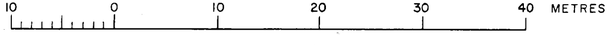

TRAVERSE PLAN

(SKETCH MAP ONLY)

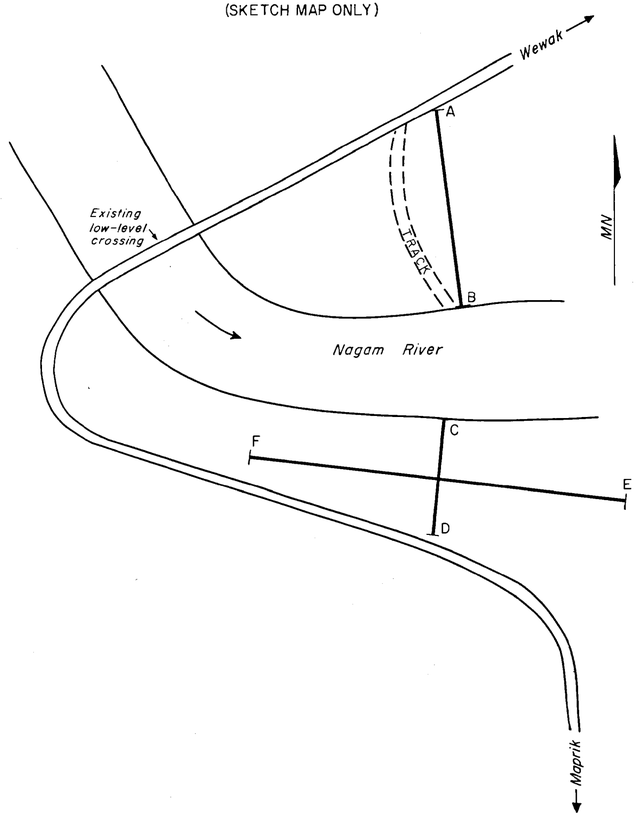

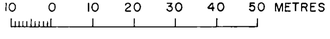

SEISMIC RESULTS—NAGAM RIVER BRIDGE SITE PNG

PLATE 21

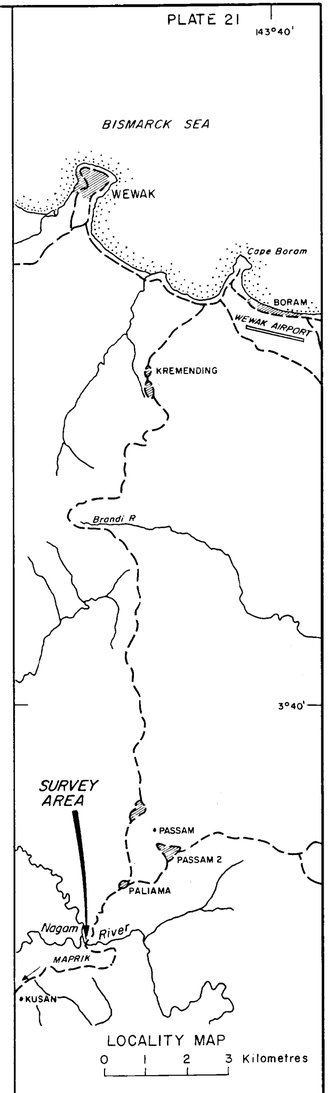

Record No. 1976/61

A54/B5-20